



## Why is unemployment so countercyclical? ☆

Lawrence J. Christiano<sup>a</sup>, Martin S. Eichenbaum<sup>a,\*</sup>, Mathias Trabandt<sup>b,c</sup>

<sup>a</sup> Northwestern University, Department of Economics, 2001 Sheridan Road, Evanston, IL 60208, USA

<sup>b</sup> Goethe University Frankfurt, Theodor-W.-Adorno-Platz 3, 60323 Frankfurt am Main, Germany

<sup>c</sup> Halle Institute for Economic Research (IWH), Germany



### ARTICLE INFO

#### Article history:

Received 14 January 2020

Received in revised form 5 April 2021

Available online 11 May 2021

#### Keywords:

Unemployment volatility

Wage inertia

### ABSTRACT

We argue that wage inertia plays a pivotal role in allowing empirically plausible variants of the standard search and matching model to account for the large countercyclical response of unemployment to shocks.

© 2021 The Authors. Published by Elsevier Inc. This is an open access article under the CC BY license (<http://creativecommons.org/licenses/by/4.0/>).

## 1. Introduction

Wage rigidities play a critical role in many quantitative business cycle models. Estimated New Keynesian (NK) models consistently feature important nominal wage rigidities.<sup>1</sup> The newest generation of heterogeneous agent New Keynesian (HANK) models also assigns a prominent role to wage rigidities.<sup>2</sup> Finally, there is a long tradition of wage rigidities in open-economy models of aggregate fluctuations.<sup>3</sup> Wage rigidities enable all of these models to generate employment fluctuations that are comparable to those observed in the data.

But do wage rigidities play an important role in understanding why unemployment is so countercyclical? The standard framework used to study unemployment features search and matching frictions of the sort emphasized by Diamond (1982), Mortensen (1982) and Pissarides (1985) (henceforth, DMP). Shimer (2005) showed that standard versions of these models cannot – at least with plausible parameter values – explain the countercyclical behavior of unemployment. This “Shimer critique” has led to a very large literature whose goal is to account quantitatively for the dynamics of unemployment. Within this literature there is disagreement about the role of wage inertia in the cyclical behavior of unemployment.

Authors such as Hall (2005) and Rogerson and Shimer (2011) argue that wage inertia greatly increases the cyclical volatility of unemployment in search and matching models. Similarly, Gertler and Trigari (2009) and Christiano et al. (2016, CET) stress the importance of wage rigidities in estimated New Keynesian search and matching models. In sharp contrast, Hagedorn and Manovskii (2008, HM) argue that wage rigidity plays only a very small role. We explain why we disagree with them. Ljungqvist and Sargent (2017) (LS) acknowledge that wage inertia might well contribute to labor market volatility. But

☆ We are grateful to Stefan Gebauer, Martin Harding and Sandra Pasch for helpful comments, and to Hannah Seidl for her assistance. We also thank Lars Ljungqvist and Tom Sargent for an extensive correspondence regarding the subject of this paper. We are grateful to the referee for comments that led to improvements in the paper.

\* Corresponding author.

E-mail addresses: l-christiano@northwestern.edu (L.J. Christiano), eich@northwestern.edu (M.S. Eichenbaum), mathias.trabandt@gmail.com (M. Trabandt).

<sup>1</sup> See, for example, Christiano et al. (2005) and Smets and Wouters (2007). See also Del Negro et al. (2013) for an example of dynamic stochastic general equilibrium models used for policy analysis.

<sup>2</sup> See for example Auclert et al. (2019) and Broer et al. (2020).

<sup>3</sup> See for example Kollmann (2001), Christiano et al. (2011), Schmitt-Grohé and Uribe (2016) and Eichenbaum et al. (2019).

to understand how wage inertia might do this, they argue that one must appreciate the vital role played by an object that they call the *fundamental surplus* (FS). We agree, with some caveats, that the FS can play a useful role in certain econometric settings. However, we question its general usefulness for illuminating the economic forces driving aggregate labor market volatility. In part, this limitation reflects that the FS is not uniquely defined for the models that we consider.

Using a variety of methods, we argue that wage rigidities play a pivotal role in allowing variants of the standard search and matching models to account for the large countercyclical response of unemployment to shocks. In fact, wage rigidities are necessary in empirically plausible versions of those models for explaining the cyclical volatility of unemployment.

In Section 2, we present a simple labor market search and matching model. In Section 3, we proceed as in much of the literature and use comparative steady state analysis as a shortcut for analyzing model dynamics. We characterize the implications of the search and matching model for the volatility of unemployment by a standard statistic: the elasticity of steady-state labor market tightness with respect to a shift in the steady-state marginal revenue product of labor. We decompose that elasticity into a wage inertia component and a component we call the *private fundamental surplus* (PFS). By the latter, we mean the fraction of a job's output that a firm allocates to vacancy creation. Our decomposition makes clear that wage inertia is a necessary condition for generating a large countercyclical response of unemployment to a shift in the marginal revenue product of labor. If the wage rate responds one-to-one to the marginal revenue product across steady states, then the unemployment rate remains exactly the same across those steady states. Our decomposition also makes clear that, other things equal, the less the wage rate responds to the marginal revenue product, the more responsive is the unemployment rate.

We apply our decomposition to analyze the role of wage inertia in different wage-setting models estimated by CET. Specifically, we consider versions of their DSGE model in which wages are set according to Nash bargaining and alternating offer bargaining (AOB). The first model does not solve the Shimer puzzle. The second model does. We argue that the AOB model does better because it embodies more wage inertia. Does the FS shed light on this finding? As it turns out, two measures of the FS are consistent with LS's definition. Depending on which measure we adopt, the FS plays either an enormous role or a small role in explaining why the AOB model exhibits so much more labor market volatility than the Nash model.

In Section 3, we also address the HM critique of wage inertia as a solution to the Shimer puzzle. First, we analyze their argument. Second, we replace Nash bargaining by sticky wages. By the latter, we mean that wages are constant across steady states after a permanent shock to labor productivity. Under sticky wages, the model exhibits drastically higher labor market volatility.

The comparative steady-state approach can yield important insights about the role of wage rigidity in dynamics. However, it can also be misleading. The approach assumes the underlying shock is close to a random walk and the economy does not have quantitatively important state variables. These two assumptions are satisfied in the simple search and matching model (e.g., Shimer (2005)). But they are not satisfied in generalizations of that model that include transitory shocks and a rich assortment of state variables. Moreover, model features such as adjustment costs and nominal rigidities give rise to additional sources of dynamics while leaving no trace in the steady state. A steady-state analysis could assign no role at all to wage rigidity even if in fact it plays a very important role.

In light of these considerations, Section 4 focuses on the dynamic response of unemployment to shocks. We do so using variants of the Nash and AOB models estimated in CET. Our main results can be summarized as follows. Wage inertia greatly magnifies the response of unemployment to shocks. That is, models that do well at matching the data, such as the estimated AOB model, do poorly if one replaces the wage determination mechanism by one in which wages are less inertial. Models that do badly at matching the data, such as the Nash model with a plausible replacement ratio, do much better if we impose on them wage processes that are more inertial.

Section 5 contains concluding remarks.

## 2. A simple labor market model

In this section, we describe the labor market sector in the CET model. The rest of the model is described in Section 4. We proceed in this way for two reasons. First, it allows us to focus on how wages are determined. Second, it lets us highlight the subset of the steady-state equations in the CET model that we use to comment on the literature.

The size of the labor force is a constant, normalized to unity. Workers search for jobs and have a stochastic discount factor,  $m_{t+1}$ , which they take as given. We denote the probability that a worker finds a job by  $f_t$ . A continuum of firms produces a homogeneous good using labor as the sole input. In the CET model, these firms are referred to as wholesalers. For this type of firm to meet a worker in period  $t$ , it must post a vacancy that has a real cost,  $s_t$ . By a real price or cost we mean that it is expressed in units of the consumption good. A firm fills a vacancy with probability  $Q_t$ . Following Pissarides (2009), the firm must pay a fixed real cost,  $\kappa_t$ , before bargaining with the newly found worker. The firm produces one unit of the homogeneous good with one unit of labor. The firm sells that good to a competitive market at a real price,  $\vartheta_t$ . In the broader CET model,  $\vartheta_t$  is a function of all of the shocks. Firms have the same discount factor as workers.

Let  $J_t$  denote the real value to the firm of a worker:

$$J_t = \vartheta_t^p - w_t^p. \quad (1)$$

Here,  $\vartheta_t^p$  denotes the expected present discounted value of  $\vartheta_t$  over the duration of the worker-firm match. The variable  $w_t^p$  denotes the discounted value of the real wage,  $w_t$ . In recursive form:

$$\vartheta_t^p = \vartheta_t + \rho E_t m_{t+1} \vartheta_{t+1}^p, \quad w_t^p = w_t + \rho E_t m_{t+1} w_{t+1}^p, \quad (2)$$

where  $\rho$  is the probability that a given firm-worker match continues from one period to the next.

The law of motion for aggregate employment,  $l_t$ , is given by

$$l_t = \rho l_{t-1} + x_t l_{t-1}. \quad (3)$$

The term  $\rho l_{t-1}$  denotes the number of workers that were attached to firms in period  $t-1$  and remain attached at the start of period  $t$ . The variable  $x_t$  denotes the hiring rate so that  $x_t l_{t-1}$  represents the number of new worker-firm meetings at the start of period  $t$ . The number of workers searching for work at the start of period  $t$  is the sum of the number of unemployed workers in period  $t-1$ ,  $1-l_{t-1}$ , plus the number of workers that separate from firms at the end of  $t-1$ ,  $(1-\rho)l_{t-1}$ . Consequently, the probability,  $f_t$ , that a searching worker meets a firm is given by

$$f_t = \frac{x_t l_{t-1}}{1 - \rho l_{t-1}}. \quad (4)$$

Free entry by wholesalers implies that, in equilibrium, the expected benefit of a vacancy equals the cost:

$$Q_t (J_t - \kappa_t) = s_t. \quad (5)$$

Let  $V_t$  denote the value to a worker of being matched with a firm. We write  $V_t$  as the sum of the expected present discounted value of wages earned while the firm-worker match endures and the continuation value,  $A_t$ , when the match terminates:

$$V_t = w_t^p + A_t. \quad (6)$$

Here,

$$A_t = (1-\rho)E_t m_{t+1} [f_{t+1} V_{t+1} + (1-f_{t+1})U_{t+1}] + \rho E_t m_{t+1} A_{t+1}, \quad (7)$$

and

$$U_t = D_t + \tilde{U}_t, \quad (8)$$

where  $D_t$  denotes period  $t$  unemployment benefits. In addition,  $\tilde{U}_t$  denotes the continuation value of unemployment:

$$\tilde{U}_t \equiv E_t m_{t+1} [f_{t+1} V_{t+1} + (1-f_{t+1})U_{t+1}]. \quad (9)$$

Labor market tightness,  $\Gamma_t$ , is the ratio of aggregate vacancies to the number of workers searching for work. Assuming a standard constant returns to scale matching function, the vacancy-filling rate,  $Q_t$ , and the job-finding rate for workers,  $f_t$ , are related to  $\Gamma_t$  as follows:

$$f_t = \sigma_m \Gamma_t^{1-\sigma}, \quad Q_t = \sigma_m \Gamma_t^{-\sigma}, \quad (10)$$

where  $\sigma_m > 0$ ,  $0 < \sigma < 1$  and

$$\Gamma_t = \frac{v_t l_{t-1}}{1 - \rho l_{t-1}}. \quad (11)$$

Here,  $v_t l_{t-1}$  denotes the total number of vacancies posted by firms at the start of period  $t$ .

As soon as the  $l_t$  matches are determined at the start of period  $t$ , each worker in  $l_t$  engages in bilateral bargaining over  $w_t$  with a wholesaler firm. Each worker-firm bargaining pair takes the outcome of all other period  $t$  bargains as given. In addition, they take as given the outcome of future wage agreements as long as the worker and firm remain matched. Because bargaining in period  $t$  applies only to the current wage rate, we refer to it as *period-by-period bargaining*. The bargaining problem of all worker-firm pairs is the same regardless of how long they have been matched.<sup>4</sup>

In the basic search and matching model, the match surplus  $J_t + V_t - U_t$  is split between a matched firm and worker according to Nash bargaining. The Nash-sharing rule is given by

$$J_t = \frac{1-\eta}{\eta} (V_t - U_t), \quad (12)$$

<sup>4</sup> This result follows from our assumptions that hiring costs (i.e.  $s_t$  and  $\kappa_t$ ) are sunk when bargaining occurs and that the expected duration of a match is independent of how long a match has already been in place.

where  $\eta$  is the share of total surplus going to the worker.

Following Hall and Milgrom (2008) and CET, we also consider a version of the model in which real wages are determined by the following alternating offer bargaining game. We suppose that bargaining proceeds across  $M$  subperiods within the period, where  $M$  is even.<sup>5</sup> The firm makes a wage offer at the start of the first subperiod. It also makes an offer at the start of a subsequent odd sub-period in the event that all previous offers have been rejected. The cost to a firm of making a counter offer is  $\gamma_t$ . Similarly, the worker makes a wage offer at the start of an even subperiod in case all previous offers have been rejected. The worker makes the last offer, which is a take-it-or-leave-it offer. In subperiods  $j = 1, \dots, M - 1$ , the recipient of an offer has the option to accept or reject it. If the offer is rejected, the recipient may declare an end to the negotiations or may plan to make a counteroffer at the start of the next subperiod. In the latter case, with probability  $\delta$ , bargaining breaks down.

As shown in CET, the solution to the AOB problem is given by

$$w_t^p = \frac{\alpha_1 \vartheta_t^p + \alpha_2 (U_t - A_t) + \alpha_3 \gamma_t - \alpha_4 (\vartheta_t - D_t)}{\alpha_1 + \alpha_2}, \quad (13)$$

where  $\alpha_1 = 1 - \delta + (1 - \delta)^M$ ,  $\alpha_2 = 1 - (1 - \delta)^M$ ,  $\alpha_3 = \alpha_2 (1 - \delta) / \delta - \alpha_1$  and  $\alpha_4 = (1 - \delta)(\alpha_2 / M) / (2 - \delta) + 1 - \alpha_2$ . Relations (1), (6) and (13) can be combined and written in the form of the AOB-sharing rule:

$$J_t = \beta_1 (V_t - U_t) - \beta_2 \gamma_t + \beta_3 (\vartheta_t - D_t) \quad (14)$$

with  $\beta_i = \alpha_{i+1} / \alpha_1$ , for  $i = 1, 2, 3$ . The Nash-sharing rule corresponds to the expression in equation (14) with

$$\beta_1 = (1 - \eta) / \eta \text{ and } \beta_2 = \beta_3 = 0. \quad (15)$$

It is important to differentiate this “nesting” result from another well-known result. Binmore et al. (1986) describe a class of environments in which the Nash bargaining solution, equation (15), is the solution to a particular alternating offer bargaining problem. Their result requires that this alternating offer bargaining problem satisfies a particular set of bargaining protocols.<sup>6</sup> Those bargaining protocols may not correspond to the ones in our AOB model (nor does our analysis require this). As it turns out, we have had difficulty identifying a set of structural parameters (i.e., values of  $M, \delta, \gamma$ ) for which the solution to our AOB model coincides with equations (14) and (15) for any  $\eta \in (0, 1)$ . We have identified a sequence of parameterizations for our AOB model, which imply that, as  $M \rightarrow \infty$ , equations (14) and (15) are satisfied arbitrarily well for  $\eta = 1/2$ .<sup>7</sup> But this is only an isolated example. In general, the Nash model is a restricted version of the AOB model in terms of reduced-form parameters, but not necessarily in the Binmore-Rubenstein-Wolinsky sense. That is the reason why we refer to Nash and our AOB model as distinct models.

We use (2) to solve for the real wage:  $w_t = w_t^p - \rho E_t m_{t+1} w_{t+1}^p$ . In principle,  $w_t^p$  is consistent with a wide variety of wage payments over the periods in which the worker and firm remain matched. We resolve this potential non-uniqueness in  $w_t$  by assuming that each period's wage rate is the same time-invariant function of variables that are exogenous to the worker and firm.

### 3. Steady-state analysis of wage inertia and labor market volatility

In this section, we use variants of comparative steady-state methods to discuss the role of wage inertia in generating labor market volatility. We do so recognizing that these methods can potentially be misleading because many model features can have a profound impact on dynamics but leave no trace in the steady state. An additional caveat about terminology: using the term “wage inertia” in a comparative steady-state analysis is potentially confusing. In dynamic models, this term often refers to situations in which wages are slow to return to a given steady state. In this section, the term “wage inertia”

<sup>5</sup> Our model differs from Hall and Milgrom's in three ways. First, they assume alternating offers are made in successive periods,  $t, t + 1, \dots$ , and can potentially continue indefinitely. With this assumption, they must specify the time period of the model to be shorter than the quarterly or monthly rate over which many macroeconomic variables are measured. Our approach, which assumes that bargaining proceeds within a period, means that when we use standard time series estimation methods on quarterly data, as in CET, we can avoid having to explicitly take into account temporal aggregation effects. Second, we assume that a worker can go from one job to another without passing through unemployment. Third, the representative large family in our model assigns no disutility to employment (see equation (41)). Hall and Milgrom assume that employment does enter the family's utility function and show that  $D_t$  can be interpreted as the sum of unemployment benefit payments and a positive term that measures the forgone value of nonworking time. This allows them to, in effect, use a large value of  $D_t$  without violating evidence on unemployment benefits. We refer to our model as “our AOB model” rather than “the Hall and Milgrom model” to minimize confusion about the differences between the models.

<sup>6</sup> By “bargaining protocols,” we mean what is the time period over which offers and counteroffers are made, the length of time that bargaining can go on, the person who makes the first offer, the consequences of rejecting an offer, and other protocols.

<sup>7</sup> We describe a sequence of parameterizations for our AOB model as  $M \rightarrow \infty$ . Let  $\delta = 1 - \exp(-\lambda / M^\tau)$  where the power,  $\tau$ , satisfies  $0 < \tau < 1$ . So,  $\delta \rightarrow 0$  as  $M \rightarrow \infty$ . We set  $\lambda$  to what is required for  $\delta$  to take on the CET estimate of that parameter given CET's value,  $M = 60$ , and given  $\tau \in (0, 1)$ . Also, let  $\gamma = (1 - \exp(-\lambda M^{-\tau})) AM^{-\omega}$ , where  $\omega > 0$ . We can choose  $A$  so that for given  $\tau, \omega$ , and  $M = 60$ ,  $\gamma$  equals the value estimated in CET. To avoid cluttering the notation, we do not index  $\gamma, \delta$ , by  $M, \tau$  or  $\omega$ . Then, it is easily verified that  $\beta_1 \rightarrow 1, \beta_2 \gamma \rightarrow 0, \beta_3 \rightarrow 0$ . Thus, in the limit, the sequence of AOB parameterizations converges to the Nash bargaining solution with an equal bargaining share for workers and firms. In the case that  $\tau \geq 1, \beta_3$  converges to a positive number so the restriction on  $\beta_3$  in equation (15) is violated.

means that when there is a permanent shift in an exogenous variable, the wage rates in the new and old steady states do not differ very much.

Using steady-state methods, we show that the amount of labor market volatility in CET's estimated AOB model is greater than the volatility implied by what we call the *restricted Nash model*. The latter is the estimated Nash model with  $\kappa > 0$  in CET and in addition setting the value of  $D$  after the model estimation such that it is consistent with observed replacement ratios. We provide a simple steady-state-based decomposition that makes precise the notion that the relatively high labor market volatility in the estimated AOB model reflects that there is more wage inertia in that model than in the restricted Nash model.

Various authors have expressed skepticism about the role of wage inertia in determining labor market volatility. HM argue that it plays only a very small role. We explain why we disagree with them. LS argue that wage inertia might well contribute to labor market volatility. But in their view, to understand the deeper economic forces at work it is vital to appreciate the central role played by an object that they call the *fundamental surplus* (FS). We disagree and question the usefulness of the FS for illuminating the economic forces driving aggregate labor market volatility.

The problem with the LS analysis begins with the fact that they do not provide a formal economic definition of the FS. For example, they provide no analog to the type of definition we have of basic concepts in economics, such as “consumer surplus” or the “economic surplus associated with a worker-employer job match”. In practice, LS define the FS as the second factor in a two-factor multiplicative decomposition of a measure of market volatility. We show that this decomposition is not, in general, unique and gives rise to at least two measures of the FS (see Proposition 1). According to one measure, the higher labor market volatility in our AOB model relative to the restricted Nash model reflects the operation of the FS. According to the other measure, the FS plays virtually no role. So, absent a criterion for choosing between the two measures of the FS, that concept is uninformative.

Is there a criterion that allows us to focus on just one measure of the FS? If we are interested in robustly assessing the economic effects of changes in parameter values or other model features on labor market volatility, then the answer is no. If we are interested in making back-of-the-envelope guesses about the in-sample fit of various search and matching models, then the answer is a qualified yes.

The first subsection that follows describes the steady-state equilibrium of the labor market model described in Section 2 and presents our wage inertia decomposition. Subsection 3.2 discusses the parameterization of our AOB model and the restricted Nash model. Using comparative steady-state methods, we argue that the former generates more labor market volatility because it induces more wage inertia. Subsection 3.3 explains why we reach a different conclusion from HM about the impact of wage inertia. Subsection 3.4 discusses the FS.

### 3.1. A wage inertia decomposition and steady state

In this subsection, we take as given the value of the marginal product of the worker,  $\vartheta$ , which is determined in the non-labor market part of the fully specified DSGE model in Subsection 4.2. In addition, the discount factor in the steady state is  $m_{t+1} = \beta$ . The steady state of the labor market is determined by two forces: firms' free-entry condition and the wage-setting arrangement.

We begin by discussing the implications of the firm free-entry condition:

$$\frac{s}{\sigma_m} \Gamma^\sigma + \kappa = \frac{\vartheta - w}{1 - \rho\beta}. \quad (16)$$

Equation (16) is derived from equation (1) after using equations (5) and (10) to substitute for  $J$  and  $Q$ , respectively. Variables for which the time subscript has been deleted correspond to their value in the nonstochastic steady state. The right-hand side of equation (16) describes the steady-state discounted expected profits associated with a filled vacancy. It is convenient to rewrite equation (16) as follows:

$$PFS \equiv \frac{\vartheta - w - \kappa(1 - \rho\beta)}{\vartheta} = (1 - \rho\beta) \frac{s}{\vartheta Q} > 0. \quad (17)$$

The first equality defines the PFS as the fraction of a worker's output, after netting out the wage and the annuitized fixed cost of hiring, relative to the worker's output. The second equality is the zero profit condition implied by the assumption of free entry: the PFS is equal to the (annuitized) vacancy-creation cost of the match, scaled by  $\vartheta$ .

Denote the elasticity of market tightness with respect to the marginal revenue product,  $\vartheta$ , by  $\eta_{\Gamma, \vartheta}$ :

$$\eta_{\Gamma, \vartheta} \equiv \frac{d \log \Gamma}{d \log \vartheta}. \quad (18)$$

Shimer (2005) and much of the related literature use the *tightness elasticity*,  $\eta_{\Gamma, \vartheta}$ , as a measure of the labor market volatility implied by a model. In part, this is motivated by simulations reported in Shimer (2005, section E), which show that  $\eta_{\Gamma, \vartheta}$  is a good indicator of labor market volatility when there are stochastic fluctuations in  $\vartheta$ . These simulations were done using what we call the *benchmark Nash model*, which is the model with Nash bargaining and  $\kappa = 0$ .

Totally differentiating (16) and rewriting yields

$$\eta_{\Gamma, \vartheta} = \frac{1}{\sigma \times PFS} \underbrace{\left[ 1 - \frac{dw}{d\vartheta} \right]}_{\text{Wage inertia}}. \quad (19)$$

Equation (19) decomposes  $\eta_{\Gamma, \vartheta}$  into a term that reflects the inverse PFS and a term that is a function of our steady-state measure of wage inertia,  $[1 - dw/d\vartheta]$ . Note that equation (19) uses only the free-entry condition, so that it holds regardless of how wages are determined. Other things equal, a wage determination mechanism that implies greater wage inertia implies a larger value of  $\eta_{\Gamma, \vartheta}$ . The intuition is simple. When the wage rate is more inertial, firms receive a greater share of the rent associated with vacancies after a rise in the marginal revenue product (or technology)  $\vartheta$ . So the more inertial is the wage, the greater is the incentive of the firm to post vacancies in the wake of an increase in  $\vartheta$ . This increased incentive leads to a greater increase in market tightness and a larger drop in unemployment after an increase in  $\vartheta$ .

Expression (19) makes clear that whatever wage determination mechanism one uses to close the model, it must deliver at least some wage inertia for the model to have a large value of  $\eta_{\Gamma, \vartheta}$ . If, across steady states, a change in  $\vartheta$  is fully reflected in the real wage rate ( $dw/d\vartheta = 1$ ), then  $\eta_{\Gamma, \vartheta}$  must be zero. However, conditional on having some wage inertia (i.e.,  $1 - dw/d\vartheta > 0$ ), additional wage inertia is neither necessary nor sufficient to have a high value of  $\eta_{\Gamma, \vartheta}$ . For example, wage inertia could be at its maximum of 1 and  $\eta_{\Gamma, \vartheta}$  might still be small if  $PFS$  is large. So, it is an open question when a model adjustment succeeds in producing a higher value of  $\eta_{\Gamma, \vartheta}$ , whether it does so primarily by increasing wage inertia or by another means. We will show that labor market volatility in our estimated AOB model is higher than it is in the restricted Nash model because wages are more inertial in the AOB model.

In the case of AOB bargaining, the wage-setting arrangement is characterized by the steady-state version of the sharing rule, equation (14):

$$\frac{s}{\sigma_m} \Gamma^\sigma + \kappa = \beta_1 S^w - \beta_2 \gamma + \beta_3 (\vartheta - D), \quad (20)$$

where equation (5) has been used to substitute for  $J$ . Here,  $S^w$  denotes the steady-state match surplus,  $V_t - U_t$ , enjoyed by the worker:

$$S^w = \frac{w - D}{1 - \rho\beta(1 - \sigma_m \Gamma^{1-\sigma})}, \quad (21)$$

where  $f = \sigma_m \Gamma^{1-\sigma}$  represents the job-finding rate by equation (10).

An interior steady state of the model is a set of positive values of  $\Gamma$ ,  $S^w$ ,  $w$ ,  $f$ ,  $Q$  that satisfy (i) equations (16), (20), (21) and the steady-state versions of the two expressions in equation (10); and (ii)  $f, Q \in (0, 1)$ .

In the case of Nash bargaining, the steady-state version of the surplus sharing rule in equation (12) is

$$\frac{\vartheta - w}{1 - \rho\beta} = \frac{1 - \eta}{\eta} S^w. \quad (22)$$

Here,  $\eta$  denotes the share of total surplus,  $J + S^w$ , enjoyed by the worker. An interior steady state is a set of positive values of  $\Gamma$ ,  $S^w$ ,  $w$ ,  $f$ ,  $Q$  that satisfy (i) equations (22), (21), (16) and the two conditions in equation (10); and (ii) the relevant non-negativity and inequality constraints. For later purposes, it is convenient to solve equation (22) for  $\eta$  after using equation (21) to substitute for  $S^w$ :

$$\eta = \frac{w_\vartheta (1 - D_w) \frac{1 - \rho\beta}{1 - \rho\beta(1-f)}}{1 - w_\vartheta + w_\vartheta (1 - D_w) \frac{1 - \rho\beta}{1 - \rho\beta(1-f)}}, \quad (23)$$

where  $w_\vartheta \equiv w/\vartheta$  and  $D_w \equiv D/w$ .

In the case of the sticky wage model, the wage rate,  $w$ , is a model parameter and we solve for  $\Gamma$  and  $S^w$  using equations (16) and (21), respectively.

### 3.2. Quantitative role of wage inertia in the CET empirical analysis

In this section, we use the decomposition in equation (19) to quantify the role of wage inertia in raising the elasticity of market tightness in the estimated AOB model relative to the restricted Nash model. Since an analysis of this type inevitably depends on the numerical values assigned to model parameters, we begin with a brief discussion of the estimated parameters, the model steady-state properties and their relation to those in the literature. Details about the Bayesian procedure used to estimate the model can be found in CET.

Model parameters are summarized in Table 1. Consider first the parameters of the AOB model. When estimating that model, CET adjust the values of  $\sigma_m$  and  $\gamma$  so that, conditional on the other model parameters, the steady-state unemployment rate,  $1 - l$ , is 5.5 percent<sup>8</sup> and the steady-state vacancy-filling rate,  $Q$ , is 0.7.<sup>9</sup>

Some model parameters were set a priori. For example, CET simply set  $\beta$  so that the annual utility discount rate is 3 percent in the steady state. Also, during estimation CET keep the value of the quarterly match survival rate,  $\rho$ , fixed at the value reported in Shimer (2005, p. 38). The value of

$$f = (1 - \rho)l / (1 - \rho l) \quad (24)$$

follows immediately from the steady-state version of equations (3) and (4) and the assumed values of  $l$  and  $\rho$ .

In the AOB model, the outside option of a worker,  $D$ , is an unemployment benefit payment. Our value of  $D_w$  is slightly below the value of 0.4, which Shimer (2005, p. 38) argues “...lies at the upper end of the range of income replacement rates in the United States if interpreted entirely as an unemployment benefit.”<sup>10</sup> Our estimated value of  $w_\vartheta$  coincides, after rounding, to the empirical estimate of that object reported in Shimer (2005, p. 38).<sup>11</sup>

CET set  $M = 60$ , so that, given the quarterly time period in the model, offers and counteroffers are made from one day to the next, as in Hall and Milgrom (2008). The value of  $\gamma$  implies that it costs a firm 59 percent of one day’s output per worker,  $\vartheta/M$ , to make a counteroffer. This value is somewhat larger than the one assumed by Hall and Milgrom (2008, p. 1664), which implies that it costs 23 percent of a day’s production by one worker for a firm to make a counteroffer.

Consider  $\delta$ , the probability of bargaining breaking down on a day when an offer or counteroffer is refused. CET’s estimate of  $\delta$ , 0.002, is somewhat lower than the value of 0.0055 adopted in Hall and Milgrom (2008, p. 1665). CET’s estimated value of  $\sigma$  is roughly the same as the value of 0.5 chosen by Hall and Milgrom (2008, p. 1665). CET’s estimated value of the fixed cost of hiring,  $\kappa$ , implies that in the steady state, 93 percent of the cost of hiring a worker is accounted for by the fixed cost. In contrast, Hall and Milgrom (2008) assume that  $\kappa = 0$ .

In the estimated AOB model, 93 percent of the match surplus goes to workers. This percentage is substantially larger than the analog percentage, 54 percent, in Hall and Milgrom (2008) and Mortensen and Pissarides (1994).<sup>12</sup> About half of the difference in match surplus reflects the different values assigned to  $\delta$  and  $\gamma$ . If we set these parameters to the values in Hall and Milgrom, then the share of surplus going to the worker in our AOB model falls to 75 percent. But, the corresponding elasticity of market tightness,  $\eta_{\Gamma, \vartheta}$ , then falls from 24.2 to 3.38, which is well below the empirically reasonable range. Much of this impact on  $\eta_{\Gamma, \vartheta}$  comes from  $\delta$  alone. Simply raising the value of  $\delta$  in our AOB model to 0.0055 drives  $\eta_{\Gamma, \vartheta}$  down to 6.7. Later on, we discuss the significance of the quantitative importance of the parameter  $\delta$  in our model. Although the share of the surplus going to workers is high in our AOB model relative to previous literature, we know of no direct empirical observations that contradict such a high share.

Next, consider the restricted Nash model in Table 1. CET first estimate the Nash model including the parameter  $D$ . In estimating that model, the parameters  $\sigma_m$  and  $\eta$  are adjusted so that, conditional on the other model parameters, the target values of  $1 - l$  and  $Q$  used in the AOB model are attained. Because CET impose the same value for  $\rho$  as in the estimated AOB model, the value of  $f$  is also the same across the two models. The posterior mode of  $D_w$  is 0.88, a value we consider to be implausibly high. The *restricted Nash model* is this estimated model with the value of  $D$  adjusted so that  $D_w = 0.37$ , its value in the AOB model. To keep the value of  $f$  unchanged, CET adjust  $\sigma_m$  and  $\eta$  to keep  $f$  and  $Q$  unchanged.

The value of  $\eta$  in the restricted Nash model is 0.914, which is larger than the values used in Shimer (2005) and HM. The high value of  $\eta$  is not an artifact of our estimation strategy. Conditional on our model, standard estimates of the relevant data moments reported in the literature also imply a high value of  $\eta$ . The steady-state relationship, equation (23), expresses  $\eta$  as a function of  $D_w$ ,  $w_\vartheta$ ,  $\beta$ ,  $\rho$  and  $f$ . The values for the first four variables that we use are very similar to the ones reported in Shimer (2005, p. 38):  $w_\vartheta = 0.993$ ,  $D_\vartheta = 0.4$ ,  $\rho = 0.9$  and  $\beta = 0.9881$ .<sup>13</sup> The steady state value of  $f$  in our model follows from the value of  $\rho$  and the steady state value of unemployment (see equation (24)). We set the latter variable to a value taken from the literature (see footnote 8). Evaluating equation (23) at these values of  $D_w$ ,  $w_\vartheta$ ,  $\beta$ ,  $\rho$  and  $f$ , we obtain  $\eta = 0.93$ . This value is very close to the value of  $\eta$  in our restricted Nash model.

Table 1 reports that the market tightness elasticity,  $\eta_{\Gamma, \vartheta}$ , in the estimated AOB model is 24.2, which is much larger than its value of 3.97 in the restricted Nash model. To quantify the channels by which the estimated AOB model generates a

<sup>8</sup> This value of steady-state unemployment is also targeted by Shimer (2005), HM and Hall and Milgrom (2008, p. 1664).

<sup>9</sup> See  $\lambda^f$  in den Haan et al. (2000, p. 490).

<sup>10</sup> Hall and Milgrom (2008) argue that a more empirically plausible estimate of benefit payments puts its value at one-quarter of the wage. Hall and Milgrom (2008, p. 1663) argue that unemployment benefits in their model should be assigned a value lower than the statutory level on which Shimer (2005, p. 38) bases his estimate because “...a significant fraction of the unemployed do not receive any benefit.” To the extent that this low uptake rate is concentrated among the short-term unemployed, our model captures the low uptake rate explicitly. In our model, a fraction,  $f$ , of the  $(1 - \rho)l$  workers that separate from their jobs in a quarter find new jobs within the same quarter without receiving any unemployment benefits. This may justify using the relatively high value of benefits reported in Shimer (2005) to assess the value of  $D$  estimated for our AOB model using aggregate data and simply imposed in our restricted Nash model.

<sup>11</sup> Our value of  $w_\vartheta$  is also similar to the calibrated value of that variable in Hall and Milgrom (2008, p. 1663).

<sup>12</sup> See Hall and Milgrom (2008, Table 2).

<sup>13</sup> The parameters  $\rho$  and  $\beta$  are expressed in quarterly rates.

**Table 1**  
Estimated parameters and implied steady states in AOB and restricted Nash models.

| Variable                          | Alternating offer bargaining | Restricted Nash bargaining | Description  |
|-----------------------------------|------------------------------|----------------------------|--|
| <b>A. Model Parameter Values</b>  |                              |                            |  |
| $\vartheta$                       | 0.910                        | 0.844                      | Marginal revenue product                           |
| $D$                               | 0.33                         | 0.31                       | Unemployment benefits                              |
| $\kappa$                          | 0.057                        | 0.072                      | Fixed hiring cost                                  |
| $\sigma$                          | 0.552                        | 0.542                      | Matching function parameter                        |
| $\rho$                            | 0.900                        | 0.900                      | Job survival probability                           |
| $\beta$                           | 0.9968                       | 0.9968                     | Discount factor                                    |
| $\eta$                            | -                            | 0.914                      | Worker bargaining power                            |
| $\delta$                          | 0.002                        | -                          | Prob. of bargaining breakdown                      |
| $\gamma$                          | 0.009                        | -                          | Firm counteroffer costs                            |
| $M$                               | 60                           | -                          | Max. bargaining rounds                             |
| $\sigma_m$                        | 0.662                        | 0.662                      | Matching function parameter                        |
| $s$                               | 0.003                        | 0.001                      | Vacancy posting cost                               |
| <b>B. Steady-State Properties</b> |                              |                            |  |
| $D_w$                             | 0.37                         | 0.37                       | Unemployment benefits/equilibrium wage             |
| $w_\vartheta$                     | 0.993                        | 0.837                      | Real wage, relative to productivity                |
| $Q$                               | 0.7                          | 0.7                        | Vacancy-filling probability                        |
| $f$                               | 0.632                        | 0.632                      | Job-finding rate                                   |
| $l$                               | 0.945                        | 0.945                      | Employment   |
| $\eta_{\Gamma, \vartheta}$        | 24.2                         | 3.97                       | Tightness elasticity                               |
| $\kappa / (\frac{s}{Q} + \kappa)$ | 0.932                        | 0.972                      | Share of fixed cost in total cost of hiring worker |
| $\gamma / (\vartheta / M)$        | 0.593                        | -                          | Counteroffer cost as fraction of daily production  |
| $S^w / (J + S^w)$                 | 0.933                        | 0.914                      | Worker's share of total surplus                    |

Notes: For model specifications where particular parameter values are not relevant, the entries in this table are blank. Source: CET. Recall from the text, that  $D_w \equiv D/w$  and  $w_\vartheta \equiv w/\vartheta$ .

higher value of  $\eta_{\Gamma, \vartheta}$  than the restricted Nash model, we evaluate the components of equation (19) in each of the AOB and estimated restricted Nash models. Taking the ratio of the results:

$$\begin{aligned}
 6.08 &= \frac{\eta_{\Gamma, \vartheta}^{AOB}}{\eta_{\Gamma, \vartheta}^{Nash}} = \frac{1}{\sigma^{AOB}} \times \overbrace{\left[ \frac{\left( \frac{\vartheta}{\vartheta - w - \kappa(1 - \rho\beta)} \right)^{AOB}}{\left( \frac{\vartheta}{\vartheta - w - \kappa(1 - \rho\beta)} \right)^{Nash}} \right]}^{\text{PFS component}} \times \overbrace{\left[ \frac{\left[ 1 - \frac{dw}{d\vartheta} \right]^{AOB}}{\left[ 1 - \frac{dw}{d\vartheta} \right]^{Nash}} \right]}^{\text{wage inertia component}} \\
 &= 0.98 \times 0.53 \times 11.6.
 \end{aligned}$$

Here, the superscripts indicate the relevant model, as parameterized in Table 1. The roughly sixfold rise in the market tightness elasticity is more than fully accounted for by a rise in the wage inertia component. The latter rises by a factor of 11. The PFS component actually contributes to a fall in  $\eta_{\Gamma, \vartheta}$  because  $w^{AOB} > w^{Nash}$ . We conclude that wage inertia plays a critical role in allowing the estimated AOB model to generate much more labor market volatility than the restricted Nash model.

### 3.3. Wage inertia and Hagedorn and Manovskii (2008)

In this section, we address HM's conclusion that wage inertia has very little impact on labor market volatility, as measured by  $\eta_{\Gamma, \vartheta}$ . We argue that this conclusion is an artifact of the way in which HM introduce wage inertia into the model: they do so in a way that generates other effects on  $\eta_{\Gamma, \vartheta}$  that roughly cancel out the effect of wage inertia per se.

HM maintain the assumption of Nash bargaining. Given this assumption, they increase wage inertia by decreasing workers' bargaining power. That decrease leads to a decline in the wage level toward the outside option,  $D$ . Of course, when  $w = D$ , the wage is pinned down by workers' outside option, so that  $1 - dw/d\vartheta = 1$ . Our decomposition of  $\eta_{\Gamma, \vartheta}$  in (19) shows that, other things equal, a drop in the wage rate increases  $\eta_{\Gamma, \vartheta}$ . On net, the fall in the wage and the rise in wage rigidity roughly cancel each other out in terms of the impact on  $\eta_{\Gamma, \vartheta}$ . HM's analysis does not tell us what the impact of wage inertia per se is on volatility.

To evaluate the role of wage inertia per se on  $\eta_{\Gamma, \vartheta}$  we use the decomposition in equation (19) and calculate what happens to  $\eta_{\Gamma, \vartheta}$  if we assume  $dw/d\vartheta = 0$ . We keep the wage fixed at its steady-state value in the restricted Nash bargaining model. We find that  $\eta_{\Gamma, \vartheta}$  goes from 3.97 to 7225.2. Since  $\sigma$  and the PFS are held fixed in this experiment, all of the enormous increase in  $\eta_{\Gamma, \vartheta}$  is due to wage inertia.

Our decomposition of  $\eta_{\Gamma, \vartheta}$  in equation (19) abstracts from how wages are set. So these results show that if the Nash bargaining arrangement is replaced by another arrangement that leaves the PFS unchanged and increases wage inertia, then labor market volatility would rise by a lot.

### 3.4. Fundamental surplus-based decompositions

LS do not offer a formal definition of the FS. They say that the FS is “the upper bound on the fraction of a job’s output that the invisible hand can allocate to vacancy creation.” Although the owner of the “invisible hand” is the primary actor in the LS analysis, that agent’s objectives and constraints are never defined and these things are simply left to the imagination of the reader. Does the owner of the invisible hand solve some sort of Ramsey problem? Can the invisible hand choose bargaining protocols or unemployment compensation? LS offer no guidance on the answers to these types of questions.

In practice, LS measure the FS as the inverse of the second factor in a two-factor multiplicative decomposition of the tightness elasticity:

$$\eta_{\Gamma, \vartheta} = \Upsilon \times \frac{1}{FS}, \quad FS = \frac{\vartheta - x}{\vartheta}. \quad (25)$$

Here,  $\Upsilon > 0$  is a function of model parameters including the job finding rate,  $f$ . This decomposition was derived for the benchmark Nash model by Shimer (2005) and HM. In their case,  $x = D$ , the flow value of the worker’s outside option. Shimer (2005) and HM show that  $\Upsilon$  has an upper bound of roughly 2 for reasonable parameter values. Shimer (2005) and HM infer from equation (25) that, conditional on remaining within the benchmark Nash framework, the only way to raise  $\eta_{\Gamma, \vartheta}$  to the value of 20 that Shimer (2005) deems to be empirically plausible, is to set  $D$  close to  $\vartheta$  and make the inverse FS very large. However, the value of  $D$  required to put  $\eta_{\Gamma, \vartheta}$  into the empirically plausible range is far too big in light of the data.<sup>14</sup> The simplicity and transparency of this observation is part of the reason that the *Shimer puzzle* has had such a large impact on the search and matching literature.

LS argue that the type of reasoning applied in Shimer (2005) and HM generalizes to a wide range of models. For example, LS consider the Nash model with  $\kappa > 0$  as well as Hall and Milgrom (2008)’s model. Consistent with LS, a decomposition like equation (25) exists for the AOB and Nash models presented in the previous section, in which  $x$  is defined as follows:

$$x = D + \tau_{\kappa} \kappa + \tau_{\gamma} \gamma, \quad (26)$$

where  $\tau_{\kappa}, \tau_{\gamma} > 0$ .

Suppose that the decomposition satisfies the following desiderata: (i)  $\Upsilon \geq 0$  in equation (25) has a relatively low upper bound for all reasonable values of the model parameters<sup>15</sup>; (ii) the objects,  $\tau_{\kappa}, \tau_{\gamma} \geq 0$  in equation (26) are not functions of  $D, \gamma, \kappa$ ; and (iii)  $D, \gamma, \kappa$  are the key parameters that can make  $\eta_{\Gamma, \vartheta}$  large and the primary channel by which they affect  $\eta_{\Gamma, \vartheta}$  is via the uniquely-specified  $x$ . If these properties are satisfied, equation (25) represents a very simple and transparent decomposition that supports the *LS narrative*: for a model change to substantially increase  $\eta_{\Gamma, \vartheta}$ , it must substantially increase the inverse FS by setting  $x$  close to  $\vartheta$ . Notably, under (i) and (ii),  $D, \gamma$  and  $\kappa$  are perfect substitutes for making  $\eta_{\Gamma, \vartheta}$  large.

Shimer (2005) and HM show that the three desiderata hold when applied to the benchmark Nash model.<sup>16</sup> So, the LS narrative applies to that model. But the story becomes far more complicated as soon as we take even a small step away from that model (e.g., the Nash model with  $\kappa > 0$  or our AOB model). The fundamental problem is that, generically, for a given  $\eta_{\Gamma, \vartheta}$  there are two decompositions of the form given by (25). Neither of these decompositions satisfies desiderata (i)-(iii).

As noted above, the failure to define the ‘invisible hand’ forces us to approach the FS analysis from a technical perspective by focusing on the FS as a factor in a two-factor decomposition. The simplest way to illustrate the absence of economics as a guide in the analysis is provided by the Nash model with  $\kappa > 0$ , in which  $x = D + \tau_{\kappa} \kappa$ . In our AOB model,  $\kappa$  is a fixed cost that is paid before bargaining, but another possibility is that  $\kappa$  is paid after bargaining.

In our illustration, we ignore the multiplicity issue by simply focusing on the decomposition used in LS. According to LS the elasticity of market tightness,  $\eta_{\Gamma, \vartheta}$ , is inversely related to the ‘fundamental surplus’,  $\vartheta - x$ . On the surface, it feels reasonable that we need to subtract the workers’ outside option,  $D$ , from  $\vartheta$  to obtain the fundamental surplus. LS argue that an additional deduction is required to cover  $\kappa$ . In the case where  $\kappa$  is paid after bargaining, they argue that the appropriate deduction is the annuity value of  $\kappa$ ,  $(1 - \rho\beta)\kappa$ .<sup>17</sup> Our assumption that the firm pays  $\kappa$  before bargaining puts the firm in a weaker bargaining position. This is because our assumption implies that  $\kappa$  is sunk at the time of bargaining, so that the surplus to be divided at that point is higher by  $\kappa$ . As a result, the worker gains  $\eta\kappa$  in surplus and the firm (taking into account that it must pay  $\kappa$  before bargaining) loses  $\eta\kappa$ . So from an ex ante perspective, when the firm makes its vacancy posting decision the firm in effect treats  $\kappa$  as more burdensome. LS assert in their online appendix that the ‘invisible

<sup>14</sup> HM literally work with equation (25), though in different notation (see equation (1), Section II (b) of HM). Shimer (2005, p. 36) has essentially the same argument as HM. Noting that what we call  $\eta_{\Gamma, \vartheta}$  is the product of the inverse FS and the elasticity of  $\Gamma$  with respect to  $\vartheta - D$ , and that  $\Upsilon$  cannot plausibly be greater than 2, Shimer (2005, p. 36) concludes that “...unless the value of leisure [ $D$ ] is close to labor productivity [ $\vartheta$ ], the [labor market tightness,  $\Gamma$ ] is likely to be unresponsive to changes in [ $\vartheta$ ]” (square bracketed terms added by us to convert the language into our notation).

<sup>15</sup> By “relatively low upper bound”, in practice we (following LS) mean that  $\Upsilon$  can be no greater than roughly 2. This means that the only way to get  $\eta_{\Gamma, \vartheta}$  into the empirically reasonable range is to raise the inverse FS. By “reasonable values for the model parameters” we mean two things. First, model parameters must satisfy non-negativity constraints and have the property that there exists an interior equilibrium with  $f, Q \in (0, 1)$ . Second, by a “reasonable” parameter value we mean a value that numerous researches agree is justified by the data.

<sup>16</sup> Note that uniqueness of the decomposition is obvious when  $\kappa = \gamma = 0$ .

<sup>17</sup> See their Table 1.

hand' computes the fundamental surplus in this case by internalizing the firm's loss. That is, he/she/it subtracts more than the annuity value of  $\kappa$  from  $\vartheta$ ,  $[(1 - \rho\beta)/(1 - \eta)]\kappa$ , to obtain the fundamental surplus. Why the correct adjustment is specifically division by  $1 - \eta$  is not explained, though it feels right to not adjust at all when the share of surplus going to workers,  $\eta$ , is zero. Still, the adjustment is very large in our formulation of the Nash model because, given the data, that model implies a high value of  $\eta$  (see section 3.2 for a detailed discussion).

But, now we come to the crux of the economic problem. While they feel plausible, we have no economic idea of why the subtractions described above are done because the agent doing the subtraction, the owner of the 'invisible hand', is never identified. A common interpretation of the invisible hand is that it is a metaphor for the idea that people maximizing their private objectives in free markets are in fact led, 'as if by an invisible hand', to promote the public welfare. Under this interpretation, the invisible hand belongs to a benevolent planner. What are the objectives and constraints of that planner? Wouldn't such a planner be unrestricted (as in the Hosios reasoning) by the bargaining protocols? If so, why does the planner have a discontinuous policy rule that subtracts one amount corresponding to  $\kappa$  if the fixed cost occurs in the moment before the customary time for bargaining and potentially a very different amount if the fixed cost occurs in the moment after? Without a full explanation of the agent whose invisible hand is guiding events, the economic content of the analysis is unclear.

In the next subsection, we state the multiple-decomposition problem in the form of a proposition (see Proposition 1). That the multiplicity problem is quantitatively large in empirically reasonable examples is demonstrated in Subsection (3.4.2). In Subsection (3.4.3), we explore possible resolutions of the multiplicity problem. That there can be multiple two-factor decompositions of a given object is a familiar phenomenon in economics, even when one of the factors is normalized (for example, the lead coefficient in FS is unity). An example is a spectral density of a covariance-stationary stochastic process. This also has multiple two-factor representations, where the factors are functions of different moving average representations. Still, the multiplicity of moving average representations is resolved by a useful selection criterion, namely that the moving average representation be the Wold representation. We do not find a similarly-convincing resolution to the multiplicity problem in Proposition 1.<sup>18</sup>

#### 3.4.1. Multiplicity of two-factor decompositions of $\eta_{\Gamma, \vartheta}$

Here we describe, and then discuss, the multiplicity of two-factor decompositions, equations (25) and (26), for our AOB and Nash models. Consider the AOB model. A decomposition of  $\eta_{\Gamma, \vartheta}$  in equations (25) and (26) is characterized by a triple,  $(\Upsilon, \tau_\kappa, \tau_\gamma)$ . The following discussion establishes that there are at least two decompositions of  $\eta_{\Gamma, \vartheta}$ . In the *structural decomposition*,  $\tau_\kappa$  and  $\tau_\gamma$  are analytic functions of model structural parameters, not including  $D, \kappa, \gamma$ . We denote this decomposition by  $(\Upsilon^S, \tau_\kappa^S, \tau_\gamma^S)$ . This is the type of decomposition stressed in LS (see their Table 1). In the *non-structural decomposition*,  $\tau_\kappa$  and  $\tau_\gamma$  are functions of all model parameters, including  $D, \kappa, \gamma$ , because each element in the triple,  $(\Upsilon, \tau_\kappa, \tau_\gamma)$ , is a function of the equilibrium finding rate,  $f$ . We denote the elements of this decomposition by  $(\Upsilon^{NS}, \tau_\kappa^{NS}, \tau_\gamma^{NS})$ . Ljungqvist and Sargent (2021) adopt this type of decomposition. In both decompositions the object,  $\Upsilon$ , is a function of  $f$ .

See the Technical Appendix, Section A, for the derivation of the structural decomposition:

$$\Upsilon^S = \frac{\beta_1 + (1 - \rho\beta)\beta_3 + \rho\beta\beta_3 f}{\beta_1 + (1 - \rho\beta)\beta_3} \Xi \quad (27)$$

$$\Xi = \frac{(1 - \rho\beta)(1 + \beta_1) + \rho\beta f \left(1 + (\kappa + \beta_2\gamma - \beta_3(\vartheta - D)) \frac{\sigma_m}{s} \left(\frac{f}{\sigma_m}\right)^{\frac{-\sigma}{1-\sigma}}\right)}{\sigma(1 - \rho\beta)(1 + \beta_1) + \rho\beta f \left(1 + (1 - \sigma)(\kappa + \beta_2\gamma - \beta_3(\vartheta - D)) \frac{\sigma_m}{s} \left(\frac{f}{\sigma_m}\right)^{\frac{-\sigma}{1-\sigma}}\right)} \quad (28)$$

$$\tau_\kappa^S = \frac{(1 + \beta_1)(1 - \rho\beta)}{\beta_1 + (1 - \rho\beta)\beta_3}, \quad \tau_\gamma^S = \frac{\beta_2(1 - \rho\beta)}{\beta_1 + (1 - \rho\beta)\beta_3}. \quad (29)$$

Section A in the Technical Appendix also derives the following non-structural decomposition:

$$\Upsilon^{NS} = \frac{\beta_1 + \beta_3(1 - \rho\beta(1 - f))}{\psi a}, \quad (30)$$

$$\psi = \frac{\rho\beta f + \sigma(1 - \rho\beta)(1 + \beta_1)}{\rho\beta f + (1 - \rho\beta)(1 + \beta_1)}, \quad (31)$$

$$a = \beta_1 + \left(1 - \beta\rho(1 - f) + \frac{\rho\beta f(\sigma - 1)}{\psi}\right)\beta_3, \quad (32)$$

<sup>18</sup> A trivial example that illustrates the multiplicity of two-factor decompositions considers the space of numbers. For any fixed  $y$ , there are multiple settings of  $a$  and  $b$  that satisfy  $y = a \times b$ . The example illustrates why one should always be suspicious of the uniqueness of a two-factor decomposition.

$$\tau_{\kappa}^{NS} = \frac{(1 + \beta_1)(1 - \rho\beta) + \beta\rho f + \frac{\rho\beta f(\sigma-1)}{\psi}}{a}, \quad \tau_{\gamma}^{NS} = \frac{\left[1 - \beta\rho(1 - f) + \frac{\rho\beta f(\sigma-1)}{\psi}\right]\beta_2}{a}. \quad (33)$$

The  $\beta_i$ 's are defined after equation (14).

We summarize these results in the following proposition:

**Proposition 1.** Consider a set of parameters for our model with AOB bargaining for which there is an interior steady state. Let  $(\gamma^S, \tau_{\kappa}^S, \tau_{\gamma}^S)$  be defined by equations (27)-(29). Let  $(\gamma^{NS}, \tau_{\kappa}^{NS}, \tau_{\gamma}^{NS})$  be defined by equations (30)-(33). Each of these two decompositions satisfy equations (25) and (26).

Recall that Nash bargaining is a special case of AOB bargaining in the sense of equation (15). So, Proposition 1 with  $\tau_{\gamma} = \gamma = 0$  and the  $\beta_i$ 's defined in (15) also applies to Nash bargaining. For both the AOB and Nash models, Proposition 1 implies that the FS in equation (25) is ill-defined in the sense that there are, apart from isolated exceptions, at least two distinct representations of the FS.

One exception is the AOB model with  $\delta \rightarrow 0$ . If an interior steady state exists in this case, then equations (25) and (26) hold, with<sup>19</sup>

$$\Upsilon = 1/\sigma, \quad \tau_{\kappa} = 2, \quad \tau_{\gamma} = M - 2. \quad (34)$$

A general consensus about the value of  $\sigma$  places an upper bound of roughly 2 on the value of  $\Upsilon$ . In addition,  $\tau_{\gamma}$  and  $\tau_{\kappa}$  are not functions of  $D$ ,  $\gamma$  and  $\kappa$ . The three desiderata at the end of Section 3.4 are satisfied for this case. Consequently, the example is consistent with the LS narrative: the FS is well-defined and the only way to substantially increase  $\eta_{\Gamma, \vartheta}$  is to increase the inverse FS in the parameters are  $D$ ,  $\gamma$ ,  $\kappa$  and, significantly, *not*  $\delta$ . However, it is important to understand that all these results simply flow from an assumption about the value of  $\delta$ . In effect, by replacing the actual AOB model by the version with  $\delta \rightarrow 0$  corresponds to replacing the AOB model by an alternative model.

The properties of the alternative model shed little light on our estimated AOB model for at least five reasons. First,  $\delta \rightarrow 0$  is economically uninteresting because it leads to the implausible implication that workers do not care at all about the outside option when they bargain.<sup>20</sup> Second, given CET's estimated model parameters, there exists no equilibrium for  $\delta < a$  where  $a$  is a strictly positive number. Third, approximations can provide insight when the problem at hand is intractable, but, as Proposition 1 shows, there is no need for an approximation in the case of our AOB model. Fourth, the approximation with  $\delta \rightarrow 0$  is very misleading because it suggests that a two-factor decomposition of the type in equations (25) and (26) is unique, when Proposition 1 shows that in general, it is not. Finally, equation (34) does not satisfy desiderata (iii). We showed in Section 3.2 that the value of  $\delta$  is important in determining the value of  $\eta_{\Gamma, \vartheta}$ . The absence of  $\delta$  from equation (34) implies that the approximation fails to reveal the importance of a key parameter for  $\eta_{\Gamma, \vartheta}$ .

Notably, Hall and Milgrom (2008, pp. 1670-1671) raise, and then reject, the implication in equation (34) that raising  $\gamma$  in the alternating offer bargaining model is simply an alternative, more empirically palatable, way to increase  $D$  in the benchmark Nash model. Like us, they reject this interpretation on the grounds that it neglects the important role of the parameter,  $\delta$ . Like in the case of our AOB model, LS (page 2648) in effect assume away Hall and Milgrom's concerns by analyzing instead an approximation to their model in which  $\delta$  is assigned a specific value and so does not appear in the decomposition of  $\eta_{\Gamma, \vartheta}$ . As in the case of the AOB model, we suspect that it is by analyzing an approximation of the Hall and Milgrom model, rather than their model itself, that LS are able to claim that the FS is unique and satisfies all the desiderata in the Hall and Milgrom's model.

A second special case in which the two-factor decomposition of  $\eta_{\Gamma, \vartheta}$  is unique is the benchmark Nash model (i.e.,  $\gamma = \kappa = 0$ ) studied in Shimer (2005) and HM. In this case, both decompositions are identical, and equations (15), (27) and (30) imply that

$$\Upsilon^S = \Upsilon^{NS} = \frac{\eta\rho\beta f + (1 - \rho\beta)}{\eta\rho\beta f + \sigma(1 - \rho\beta)}.$$

The unique  $\Upsilon$  is bounded in a narrow region between unity (because  $\sigma < 1$ ) and roughly 2 (because  $\Upsilon$  is decreasing in  $\eta f \geq 0$  and when  $\eta f = 0$ ,  $\Upsilon = 1/\sigma$ ).<sup>21</sup> In this case, the decomposition, equation (25) with  $\kappa = \gamma = 0$ , satisfies the desiderata, (i)-(iii). So, this case is consistent with the LS narrative.

Proposition 1 shows that when the environment is extended beyond the benchmark Nash model, say by allowing for  $\kappa > 0$  or moving to the AOB model, the FS in equation (25) is no longer well-defined. Moreover, each of the two decompositions identified in Proposition 1 fails to satisfy desiderata (i) and (ii). Consider first the structural decomposition. Equation

<sup>19</sup> To see this, simply observe that  $\delta \rightarrow 0$  implies  $\beta_1 \rightarrow 0$ ,  $\beta_2 \rightarrow \frac{M-2}{2}$ ,  $\beta_3 \rightarrow \frac{1}{2}$ . It is then easy to verify that  $\tau_{\kappa} \rightarrow 2$  and  $\tau_{\gamma} \rightarrow M - 2$  in equation (29) and equation (33). The expression, (34), can be derived by differentiating equation (20), a straightforward exercise when  $\beta_1 = 0$ . This case was brought to our attention by Ljungqvist and Sargent (2021).

<sup>20</sup> Hall and Milgrom (2008) emphasize that their model is successful at raising  $\eta_{\Gamma, \vartheta}$  because it plausibly moderates the impact of a worker's outside option on bargaining. But the extreme case in which the outside option literally exerts no impact is of little economic interest.

<sup>21</sup> These observations can be found in Shimer (2005, p. 36) and Section II.B in HM.

**Table 2**  
Quantitative analysis of fundamental surplus fraction.

|  | Elasticity, $\eta_{\Gamma, \vartheta}$ | $\Upsilon$ ( $\nu_{\Upsilon}$ ) | 1/Fundamental Surplus ( $\nu_{FS}$ ) |
|--|--|---------------------------------|--------------------------------------|
| <b>A. Alternating Offer Bargaining (AOB)</b> |  |                                 |                                      |
| Structural                                   | 24.2                                   | 7.08 (67)                       | 3.41 (33)                            |
| Non-structural                               | 24.2                                   | 1.65 (23)                       | 14.7 (77)                            |
| <b>B. Restricted Nash Bargaining</b>         |  |                                 |                                      |
| Structural                                   | 3.97                                   | 2.11                            | 1.88                                 |
| Non-structural                               | 3.97                                   | 1.08                            | 3.67                                 |

Notes: The models in Panels A and B correspond to the estimated AOB and the restricted Nash models defined in the text, with parameter values reported in Table 1. Numbers in parentheses in Panel A are the accounting breakdowns,  $\nu_{\Upsilon}, \nu_{FS}$ , defined in equation 35. Thus, 67 is the percent of the rise in  $\eta_{\Gamma, \vartheta}$  accounted for by  $\Upsilon$  under the structural decomposition.

(29) implies that  $\tau_{\kappa}$  and  $\tau_{\gamma}$  satisfy (ii). However, we show in Subsection 3.4.2 that  $\Upsilon$  does not satisfy (i) in the AOB model estimated in CET. Now consider the non-structural decomposition. In all of the numerical examples that we study,  $\Upsilon$  satisfies (i).<sup>22</sup> However, equation (33) implies that  $\tau_{\kappa}$  and  $\tau_{\gamma}$  do not satisfy (ii) because these variables are functions of the equilibrium finding rate,  $f$ . The latter is a function of  $D, \kappa$ , and  $\gamma$ . In the case of the AOB model, both decompositions fail to satisfy (iii). This is because the value of  $\delta$  is an important determinant of  $\eta_{\Gamma, \vartheta}$ , while it does not enter the decomposition in a transparent way.

Consistent with the view that neither of the decompositions satisfies all three desiderata, Ljungqvist and Sargent use different decompositions in different papers. LS uses what we call the structural decomposition (see LS, Table 1 and their online appendix). In contrast, Ljungqvist and Sargent (2021) use the non-structural decomposition to analyze the role of the FS in our AOB model.

### 3.4.2. Quantitative importance of the multiplicity problem in Proposition 1

In this subsection, we quantify the implications of Proposition 1 using the parameter values for the AOB and restricted Nash models discussed in Subsection 3.2. Table 2 presents our results. We exploit the log-linearity of  $\eta_{\Gamma, \vartheta}$  in  $\Upsilon$  and  $1/FS$  to decompose the differences in  $\eta_{\Gamma, \vartheta}$  into components due to  $\Upsilon$  and  $1/FS$ . We do so with the statistics denoted  $\nu_{\Upsilon}$  and  $\nu_{FS}$ , respectively:

$$\nu_{\Upsilon} \equiv 100 \frac{\log \Upsilon^{AOB} - \log \Upsilon^{Nash}}{\log \eta_{\Gamma, \vartheta}^{AOB} - \log \eta_{\Gamma, \vartheta}^{Nash}}, \quad \nu_{FS} \equiv 100 \frac{\log (1/FS^{AOB}) - \log (1/FS^{Nash})}{\log \eta_{\Gamma, \vartheta}^{AOB} - \log \eta_{\Gamma, \vartheta}^{Nash}}. \quad (35)$$

Note that  $100 = \nu_{\Upsilon} + \nu_{FS}$ . We refer to  $\nu_{\Upsilon}$  and  $\nu_{FS}$  as the percent difference in  $\eta_{\Gamma, \vartheta}$  across the restricted Nash model and the AOB model that is accounted for by changes in  $\Upsilon$  and in the inverse FS, respectively. The values of  $\eta_{\Gamma, \vartheta}$ ,  $\Upsilon$ , the inverse FS,  $\nu_{\Upsilon}$  and  $\nu_{FS}$ , are reported in Table 2.

Consider first the non-structural decomposition. In this case, the inverse FS fits the LS narrative. Roughly 77 percent of the sixfold jump in  $\eta_{\Gamma, \vartheta}$  is due to the fourfold jump in the inverse FS. Only 23 percent of the rise in  $\eta_{\Gamma, \vartheta}$  is accounted for by the rise in  $\Upsilon$ . Moreover, the value of  $\Upsilon$  fits the pattern observed by LS in a variety of models, remaining in a fairly narrow range, roughly between 1 and 2.

Consider next the structural decomposition. Here, the FS plays a very different role in accounting for the rise in  $\eta_{\Gamma, \vartheta}$ . Only one-third is due to the rise in the inverse FS, while two-thirds is due to a sharp increase in  $\Upsilon$ .

The fact that  $\Upsilon$  goes from 2 to roughly 7 deviates sharply from the range of variation in LS's examples, all of which use the structural decomposition. As noted above, one of LS's examples is Hall and Milgrom's (2008) alternating offer bargaining model. For that model, LS derive the decomposition of  $\eta_{\Gamma, \vartheta}$  only for the special case corresponding to the analog of  $\delta \rightarrow 0$  in our AOB model. Subsection 3.4.1 shows that in this limiting case, the two decompositions in Proposition 1 coincide and  $\Upsilon = 1/\sigma = 1.81$  (see equation (34)). The results in Table 2 show how very misleading this special case is. That table reports that for our estimated AOB model,  $\Upsilon = 7.08$  in the structural decomposition.

In sum, at the point estimates of the AOB model, the two decompositions both justify the LS narrative and flatly contradict it. The non-structural decomposition implies that the rise in  $\eta_{\Gamma, \vartheta}$  going from the Nash model to the AOB model operates through an increase in the inverse FS. The structural decomposition implies that the rise happens via an increase in  $\Upsilon$ . Critically, the model itself is entirely silent on which narrative is the right one. And LS's informal definition of the FS provides no guidance on how to select between the two narratives.

<sup>22</sup> See the examples in Figs. 1, 2, 3. For more examples, see Section C in the Technical Appendix.

### 3.4.3. Assessing the LS narrative

According to the LS narrative, for a model change to substantially increase  $\eta_{\Gamma, \vartheta}$ , it *must* substantially increase the inverse FS. Proposition 1 shows that the FS is not well defined because there are two measures of the FS, one corresponding to each decomposition. In this subsection we explore two criteria that could in principle select one of the two measures of FS. One criterion simply reverse-engineers the LS narrative by asking if one of the two decompositions robustly attributes a large role to the FS in accounting for labor market volatility. The first part of this subsection demonstrates that neither measure of FS has this property. We make this argument using what we call a *principal components approach*.

We then consider an alternative approach to selecting between the two decompositions of  $\eta_{\Gamma, \vartheta}$ . This *econometric approach* focuses on the usefulness of one of the two decompositions for generating guesses about which model perturbations are likely to improve in-sample fit. This approach favors the non-structural decomposition. The LS narrative using this decomposition does offer insights. But by suggesting that important parameters such as  $D$ ,  $\gamma$  and  $\kappa$  are perfect substitutes and ignoring  $\delta$ , that narrative can be misleading and at least oversimplifies. We show how the analysis in CET illustrates these points. We describe an econometric finding in CET that is puzzling from the point of view of the non-structural FS but is transparent when impulse response functions are included in the set of diagnostic tools. Finally, we provide several examples that highlight the limitations of this decomposition for policy analysis.

*The principal components approach* The principal components approach determines if one of the factors implied by Proposition 1 consistently tracks the response of the tightness elasticity,  $\eta_{\Gamma, \vartheta}$ , to a change in model parameters or model structure. The name of this approach derives from an analogy between the “factors” in the two-factor decomposition of  $\eta_{\Gamma, \vartheta}$  and the concept of “factors” in time series analysis.

We start by analyzing the restricted Nash model with  $\kappa > 0$  and consider a range of values of  $D$  and  $\kappa$ . To apply the principal components approach, we use the following measure,  $\nu$ , of the role of the inverse FS in transmitting the effect of a change in a model parameter into a change in  $\eta_{\Gamma, \vartheta}$ :

$$\nu = 100 \frac{\log(1/FS) - \log(1/\hat{FS})}{\log(\eta_{\Gamma, \vartheta}) - \log(\hat{\eta}_{\Gamma, \vartheta})}. \quad (36)$$

Here, the hat over  $\eta_{\Gamma, \vartheta}$  and  $1/FS$  indicates that those objects are evaluated at a set of baseline parameter values. The variables without a hat are evaluated at a point in which one parameter is perturbed from its baseline value. Let  $\nu^S$  and  $\nu^{NS}$  denote the values of  $\nu$  when FS is constructed using the structural and non-structural decompositions in Proposition 1, respectively. We compute  $\nu^S$  and  $\nu^{NS}$  on a grid of admissible values of  $\kappa$ ,  $\kappa \in [0, \bar{\kappa}]$ , where  $\bar{\kappa}$  is the value of  $\kappa$  for which  $f$  is close to zero when all other parameters (including  $D$ ) are held at their estimated values. We constructed the analogous set of admissible values for  $D$ .

In addition to displaying  $\nu^S$  and  $\nu^{NS}$ , we calculate a scalar *principal component statistic* that summarizes how well a particular factor accounts for the impact on  $\eta_{\Gamma, \vartheta}$  over the whole range of perturbations in a particular parameter. The statistic is the mean square deviation of the factor from 100 over the range of perturbations.

Section C in the Technical Appendix presents the detailed results of our experiments. Our key finding is that the measure of the inverse FS selected by the principal components approach depends on the value of  $\eta$ , the bargaining power of the worker. When  $\eta$  is equal to its estimated value (see Table 1), then the principal components method selects the inverse FS in the structural decomposition. We also consider a lower value, 0.6, of  $\eta$  and adjust  $\sigma_m$  in the restricted Nash model to keep the finding rate,  $f$ , fixed.<sup>23</sup> The value of 0.6 lies between the values in Shimer (2005, Table 2) and Hall and Milgrom (2008).<sup>24</sup> With  $\eta = 0.6$ , the principal components method selects the inverse FS in the non-structural decomposition. So, the principal components approach does not resolve the multiplicity issue raised by Proposition 1.

Next, we perform an analogous set of experiments in the AOB model. The key results can be summarized as follows. First, using the estimated AOB model, we find that the principal components statistic implies that the inverse FS in the non-structural decomposition does best on average. Recall that for the Nash model with high  $\eta$ , the principal components statistic chooses the inverse FS in the structural decomposition. So, looking across models, one cannot consistently focus on one decomposition or the other on the basis of the principal components approach.

Second, for the estimated AOB model, there are significant regions in the parameter space in which the structural decomposition measure of the inverse FS does the best job of tracking the impact of changes in  $D$ ,  $\delta$ ,  $\kappa$ ,  $\gamma$  on  $\eta_{\Gamma, \vartheta}$ . Moreover, there is a region close to the estimated parameters where  $\Upsilon$  in the structural decomposition does the best job of tracking these changes. This last result is not surprising considering the results reported in Table 2. So, looking across parameterizations of a given model, one cannot consistently focus on one decomposition or the other on the basis of the principal components approach.

Third, we analyze a version of the AOB model in which parameters are adjusted so that the share of total surplus given to labor is 0.6. In the sense of the principal components statistic, the inverse FS in the non-structural decomposition still

<sup>23</sup> We set  $\sigma_m = 0.0586$ .

<sup>24</sup> The share of surplus going to workers in Hall and Milgrom (2008) is discussed in Subsection 3.2.

does best on average in tracking  $\eta_{\Gamma, \vartheta}$ . However, behind this good average performance are some important exceptions. For example, though the impact of  $\delta$  on  $\eta_{\Gamma, \vartheta}$  is now relatively modest, the principal components criterion finds that the impact operates through  $\Upsilon$ , not through the inverse FS. Significantly, the two measures of  $\Upsilon$  offered by Proposition 1 perform about equally well in accounting for the impact on  $\delta$ .

Taken together, these results are the basis for our conclusion that the LS narrative cannot be supported once we leave the simple Nash model. Across different models and different parameterizations, different measures of the FS may work best, and sometimes  $\Upsilon$  does better than any of them.

*Econometric approach* We now turn to the second potential criterion for selecting between the two decompositions implied by Proposition 1. We find that, of the two decompositions, the non-structural is the most useful. We discuss some limitations, both for econometric analysis and for policy analysis.

### *The Non-Structural Decomposition Seems Best for Applied Econometrics*

An important part of the search and matching literature seeks to identify a model of the labor market that has good in-sample fit. The *econometric approach* selects the decomposition that is most useful for making back-of-the-envelope guesses about what model changes might improve in-sample fit. In practice, applied econometricians have strong priors over the values of some endogenous variables and weaker priors over some model parameters. For example, an econometrician might be interested in knowing how a change in  $D$  affects labor market volatility under the assumption that  $s$  or  $\sigma_m$  (or both) are adjusted to keep  $f$  unchanged. This preference could reflect that the analyst is uncertain about the value of parameters such as  $s$  or  $\sigma_m$  because of the ambiguities involved in mapping “vacancies” and, hence, “matching functions”, into data. At the same time, the econometrician might have strong views about  $f$  because it maps easily into relatively well-measured variables such as employment and unemployment.<sup>25</sup>

Under these circumstances, the econometric approach selects the non-structural decomposition. This decomposition provides a particularly convenient way to see the impact on  $\eta_{\Gamma, \vartheta}$  of a change in  $D$ ,  $\gamma$  or  $\kappa$  holding  $f$  fixed because conditional on  $f$ , the variables  $\Upsilon$ ,  $\tau_\kappa$ , and  $\tau_\gamma$  do not vary with  $D$ ,  $\gamma$  or  $\kappa$  (see equations (30)–(33)). Implicitly, the values of  $s$  and  $\sigma_m$  must be adjusted, but it is not even necessary to do that adjustment explicitly. By contrast, in the structural decomposition,  $\Upsilon$  is a function  $D$ ,  $\gamma$  and  $\kappa$  even conditional on a value of  $f$  (see equations (27)–(29)). To assess the impact of alternative values of  $D$ ,  $\gamma$  and  $\kappa$  on  $\eta_{\Gamma, \vartheta}$  using equations (25) and (26), one must recompute  $\Upsilon$ , in addition to FS.

### *Possible Advantages for FS in Applied Econometrics*

The focus of our analysis in this section has been on  $\eta_{\Gamma, \vartheta}$ . In some cases, this may be the object of intrinsic interest. But, for an econometrician seeking good in-sample fit, to be of value  $\eta_{\Gamma, \vartheta}$ , must at least be a rough indicator of the stochastic properties of a model. Some support in favor of this idea is suggested by the work in Papetti (2019) and CET.

In the case of Papetti (2019), note that if  $f$  is fixed by the choice of a combination of  $\sigma_m$  and  $s$ , then Proposition 1 implies that  $D$ ,  $\kappa$ , and  $\gamma$  are perfect substitutes in terms of  $\eta_{\Gamma, \vartheta}$ . Thus, the surface of  $\eta_{\Gamma, \vartheta}$  as a function of those three parameters is predicted to have ridges in it. Papetti (2019) shows that similar ridges appear in the posterior distribution function of the CET model. He shows this for the likelihood computed on US and Euro Area data.

CET consider what they call the *estimated Nash model*: a version of the Nash model estimated without any restriction on  $D$  or  $\kappa$ . CET find that the value of  $D$  in the estimated Nash model is implausibly high. CET (p. 1550) report that the impulse responses to the three shocks in their model are numerically nearly identical to what they are in CET’s estimated AOB model. Consequently, the log-likelihoods of the two models are essentially the same.<sup>26</sup> Interestingly, the values of  $\eta_{\Gamma, \vartheta}$  in the AOB and estimated Nash models are similar too, at 24 and 20, respectively. The magnitudes of the inverse FS (measured using the non-structural decomposition) in the estimated Nash and AOB models are also similar. This finding suggests that going from the Nash model to the AOB model in CET can be described in terms of the LS narrative. The transition involves a reallocation of the terms in  $x$  in equation (26) from  $D$  towards  $\kappa$  and  $\gamma$ . One is tempted to conclude that the AOB model simply provides an alternative interpretation, in terms of  $\kappa$  and  $\gamma$ , of the large value of  $D$  required by the estimated Nash model.<sup>27</sup>

<sup>25</sup> According to Hall and Milgrom (2008, p. 1670), “Along with virtually all researchers in the MP [Mortensen and Pissarides] and related traditions, we require that the models we consider replicate the average unemployment rate [...], which we take to be its average over the past 60 years of 5.5 percent.” (Square brackets added by us.)

<sup>26</sup> CET report that the AOB and Nash log-likelihoods are 344.6 and 343.9, respectively.

<sup>27</sup> We have motivated our interpretation of the findings in Papetti (2019) and CET by using the non-structural decomposition in the case in which the background parameters,  $\sigma_m$  and  $s$ , are adjusted to keep  $f$  and  $Q$  fixed. Our use of the non-structural decomposition is correct in that case. But both CET and Papetti (2019) adjust  $\sigma_m$  and  $\gamma$  to keep  $f$  and  $Q$  fixed. This strategy in effect makes  $\sigma_m$  and  $\gamma$  a function of the other model parameters. This is all right in the case of  $\sigma_m$  because that parameter does not appear directly in the non-structural decomposition. But  $\gamma$  obviously does (see equation (25)). As a result, the prediction of the non-structural decomposition that there is a linear tradeoff between  $D$  and  $\kappa$  in determining  $\eta_{\Gamma, \vartheta}$  is no longer true. That is because  $\gamma$  changes simultaneously with any change in  $D$  or  $\kappa$ . So, there remains room for some puzzlement over the CET and Papetti (2019) results.

Some Skepticism

There are some reasons to think that the previous argument comparing Nash and AOB models based on the FS oversimplifies.<sup>28</sup> Recall our discussion in Subsection 3.2, that the parameter  $\delta$  also plays an important role in determining  $\eta_{\Gamma,\vartheta}$  in the AOB model. But the role of  $\delta$  in the non-structural FS is not as transparent as the role of  $D, \kappa$  and  $\gamma$ . And it is hard to think about going from the Nash model to the AOB model as simply reducing the value of  $D$  and raising the value of  $\gamma$  without also considering  $\delta$ .

In our analysis, we find other reasons to be skeptical about the value of the non-structural FS as a back-of-the-envelope way of thinking about how to achieve good in-sample fit. Panel B in Table 2 reports  $\eta_{\Gamma,\vartheta}$  for the restricted Nash model, in which  $D_w$  is fixed at 0.37. Note that in that model,  $\eta_{\Gamma,\vartheta}$  has a small numerical value, even though  $\kappa > 0$ . The non-structural FS suggests that if we hold  $f$  fixed by adjusting some combination of  $\sigma_m$  and  $s$ , then we can make  $\eta_{\Gamma,\vartheta}$  arbitrarily large by simply inserting a suitably high value of  $\kappa$ .<sup>29</sup> CET estimate the Nash model adjusting  $D$  so that  $D_w = 0.37$  (call this the *estimated restricted Nash model*). In addition, they fix the values of  $f$  and  $Q$  by adjusting  $\eta$  and  $\sigma_m$ . The parameters of the estimated restricted Nash model are not substantially different from those of the restricted Nash model in Table 1.<sup>30</sup> The value of  $\kappa$  in the estimated model is slightly higher, and the value of  $\eta_{\Gamma,\vartheta}$  jumps to only 5.5. CET (p. 1552) report that the log-likelihood of the estimated restricted Nash model is a gigantic 120 log points lower than the likelihood of the estimated AOB model. They find that the key problem with the fit of the estimated restricted Nash model is that, relative to its empirical analog, the model significantly overstates the response of the real wage to an expansionary monetary policy shock. Evidently, the simple LS narrative breaks down in this example. We leave it to future work to understand the reasons for the breakdown. At this point, we see three possibilities: (i) restrictions on background parameters needed to fix  $f$  and  $Q$  are binding in CET’s computations; (ii) the background parameters used by CET are actually  $\sigma_m$  and  $\eta$ , and not the  $\sigma_m, s$  that justify relying on the non-structural decomposition; (iii) the object,  $\eta_{\Gamma,\vartheta}$ , is not nearly as good a summary of the data dynamics as, say, impulse response functions.

Limitations for Policy Analysis of Fixing  $f$

Before concluding this section, it is important to stress the limitations for policy purposes of any model analysis that holds  $f$  fixed. The obvious limitation is that it is hard to imagine a policy intervention in the labor market that is not interested in knowing the implications for  $f$  or unemployment. Still, we consider a policy maker who does not care about  $f$  and is only worried about the impact of policy on labor market volatility, measured by  $\eta_{\Gamma,\vartheta}$ . We suppose that the policy maker holds  $f$  constant and uses the non-structural decomposition for the analysis. We use our estimated AOB model to show several examples in which the policy maker even gets the sign of the response of  $\eta_{\Gamma,\vartheta}$  to a policy intervention wrong. The examples are striking because they occur at the estimated values of our parameters.

Consider a policy intervention that has the effect of increasing the fixed cost of hiring workers,  $\kappa$ . By construction, the intervention has no impact on the other parameters of the model. Fig. 1 displays, for different values of  $\kappa$ , the values of  $\eta_{\Gamma,\vartheta}$  as well as the elements of the structural and non-structural decompositions. The vertical line indicates the value of  $\kappa$  in the estimated AOB model. Note that as  $\kappa$  increases relative to its estimated value,  $\eta_{\Gamma,\vartheta}$  decreases. Suppose the policy analyst has the right model but uses the non-structural FS and fixed  $f$  to guess the impact of the policy intervention on labor market volatility. Then, equations (25) and (26) imply that  $\eta_{\Gamma,\vartheta}$  increases. Clearly, keeping  $f$  fixed would give rise to a very misleading answer about the effect of the policy intervention.

To see what is going wrong, it is useful to distinguish the direct and indirect effects of a change in  $\kappa$ . The direct effect is the one that occurs holding  $\tau_\kappa, \tau_\gamma$  and  $\Upsilon$  constant. The indirect effect arises via the effect of  $\kappa$  on  $f$  and, hence, on  $\tau_\kappa, \tau_\gamma$  and  $\Upsilon$ . The 2,1 and 2,2 panels in Fig. 1 show that  $\tau_\kappa$  and  $\tau_\gamma$  both fall in the non-structural decomposition. These indirect effects are so strong that they dominate the direct effects. That is why  $\eta_{\Gamma,\vartheta}$  decreases when  $\kappa$  increases.

Interestingly, we obtain the same results when we contemplate policy interventions that take the form of changing  $\gamma$  and  $D$ . Equations (25) and (26) imply that  $\eta_{\Gamma,\vartheta}$  is an increasing function of these parameters when  $f$  is fixed and we use

<sup>28</sup> Similar observations are made in Hall and Milgrom (2008, pp. 1670-1671). See Subsection 3.4.1.

<sup>29</sup> To see this, express the non-structural decomposition in Proposition 1 for the Nash case, with  $\kappa > 0$ :

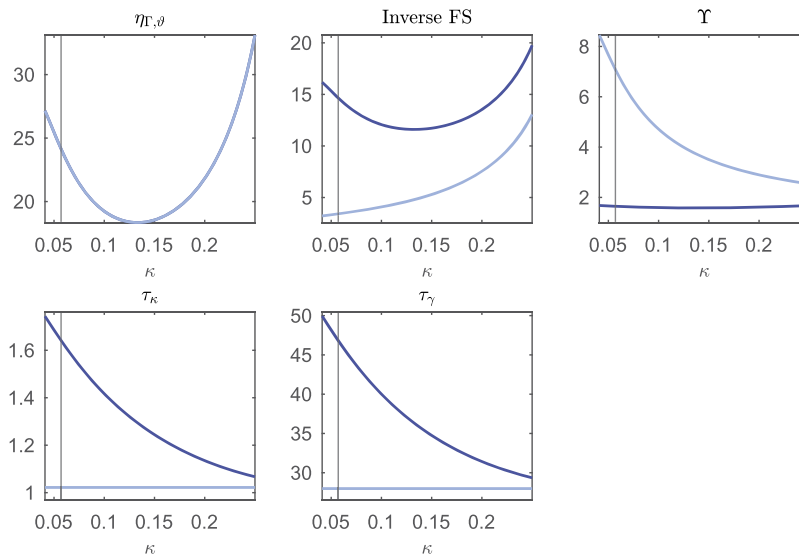
$$\eta_{\Gamma,\vartheta} = \Upsilon^{NS} \frac{\vartheta}{\vartheta - D - \tau_\kappa^{NS} \kappa}$$

$$\Upsilon^{NS} = \frac{\eta\rho\beta f + (1 - \rho\beta)}{\eta\rho\beta f + \sigma(1 - \rho\beta)},$$

$$\tau_\kappa^{NS} = \frac{1 - \rho\beta}{1 - \eta} + \frac{\eta\beta\rho f [\sigma\eta\rho\beta f + (2\sigma - 1)(1 - \rho\beta)]}{(1 - \eta)[\eta\rho\beta f + \sigma(1 - \rho\beta)]}.$$

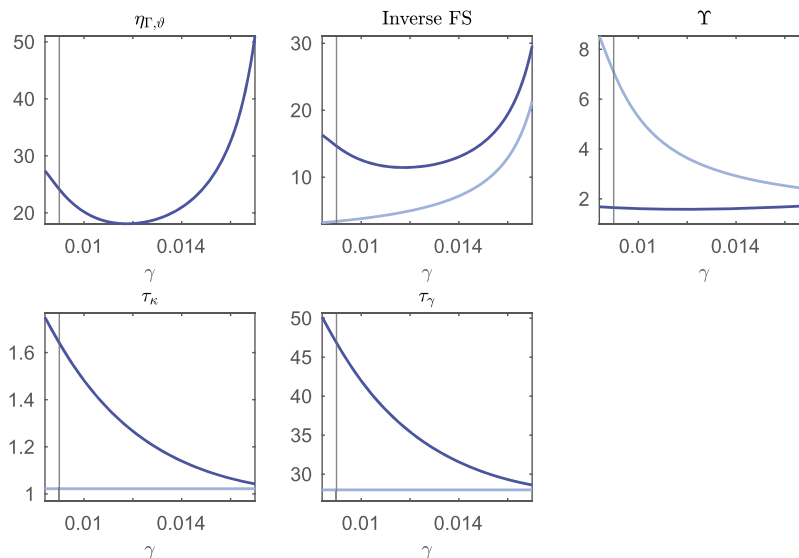
Note that  $(\Upsilon^{NS}, \tau_\kappa^{NS})$  do not depend directly on  $\sigma_m$  and  $s$ , so that we are free to adjust these to keep  $f$  fixed, as long as  $\sigma_m, s \geq 0$  and  $0 < Q < 1$ , where  $Q = \sigma_m^{\frac{1}{1-\sigma}} f^{\frac{\sigma}{1-\sigma}}$  denotes the job-matching rate.

<sup>30</sup> Details about the estimation are available from the authors on request. Needless to say, the best available methods were applied to build confidence that the actual mode of the posterior distribution was found for the estimated restricted Nash model. For example, after over 3 million draws of the MCMC algorithm, no parameterization with a higher posterior probability was found.



Notes: Elements of the two decompositions using the estimated AOB model. The light and dark curves correspond to the structural and non-structural decompositions, respectively. Vertical lines indicate the estimated value of the parameter (all the parameter values for the estimated AOB model are reported in Table 1). Calculations are based on solving the model at the indicated value of the parameter on the horizontal axis, holding fixed all other parameter values at their estimated values. Here,  $\kappa \in [0.041, 0.25]$  and  $f$  ranges from  $f = 0.92$  to  $f = 0.03$ , so that the range of values of  $\gamma$  correspond, roughly, to the admissible values of  $\gamma$  given the baseline parameterization of the AOB model in Table 1. Slightly higher values of  $\kappa$  are admissible, but they drive  $\eta_{\Gamma,\theta}$  so high that the scale in the graph is distorted.

Fig. 1. Decomposition,  $\kappa$ , in AOB model. (For interpretation of the colors in the figure(s), the reader is referred to the web version of this article.)



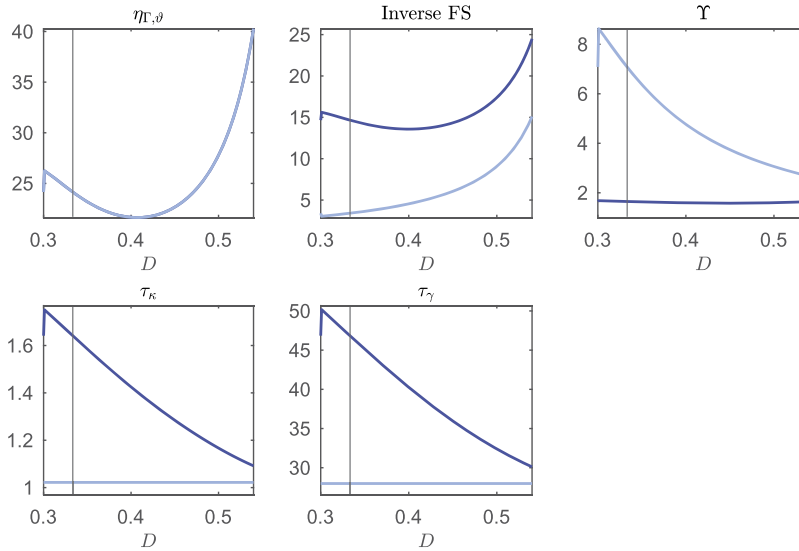
Notes: See Fig. 1. Here,  $\gamma \in [0.0084, 0.017]$  and  $f$  ranges from  $f = 0.94$  to  $f = 0.02$ , so that the range of values of  $\gamma$  corresponds, roughly, to the admissible values of  $\gamma$  given the baseline parameterization of the AOB model in Table 1.

Fig. 2. Decomposition,  $\gamma$ , in AOB model.

the non-structural decomposition. In contrast, Figs. 2 and 3 show that in a neighborhood of the estimated values of those parameters,  $\eta_{\Gamma,\theta}$  is decreasing. So, an analysis of a policy intervention that increases  $\gamma$  or  $D$  and holds  $f$  fixed would reach exactly the wrong conclusion. For additional discussion of Figs. 1, 2 and 3, see Subsection C.2.1 in the Technical Appendix.

#### 4. Dynamic analysis

In this section, we consider the dynamic impact of wage inertia in generating labor market volatility in search and matching models. We make two key points. First, comparative steady-state analysis can be deeply misleading about the dynamic behavior of these models. Models that have identical fundamental surpluses can exhibit very different dynamic



Notes: See Fig. 1. Here,  $D \in [0.30, 0.54]$  and  $f$  ranges from  $f = 0.94$  to  $f = 0.05$ , so that the range of values of  $D$  corresponds, roughly, to the admissible values of  $D$  given the baseline parameterization of the AOB model in Table 1.

Fig. 3. Decomposition,  $D$ , in AOB model.

response functions. In these cases, the fundamental surplus is uninformative about the question of interest. Second, even conditioning on a low inverse fundamental surplus, wage inertia greatly magnifies labor market fluctuations in empirically plausible versions of search and matching models. In the first subsection, we consider a simple dynamic example. In the second subsection, we analyze the impact of wage inertia in estimated DSGE models conditional on a given value of the fundamental surplus.

#### 4.1. Wage inertia: a simple dynamic example

In this section we consider the role of wage inertia using a simple dynamic example. Suppose that the equilibrium wage rate is given by the following simple inertial wage rule:

$$w_t = \phi \vartheta_t - \gamma(1 - \phi)(\vartheta_t - \vartheta), \tag{37}$$

where  $\phi > 0$  and  $D \leq w_t \leq \vartheta_t$ . In addition, assume that  $0 < \gamma(1 - \phi) < \phi$ . The latter assumption implies that a rise in  $\vartheta_t$  generates a positive response in  $w_t$ . The dynamics of  $w_t$  depend on  $\gamma$  and  $\phi$ . Note that  $\gamma$  has no impact on the steady-state value of  $w_t$ . We can think of this wage rule as being a variant of the Hall (2005) wage norm, as long as  $D \leq w_t \leq \vartheta_t$  so that the firm and worker each have an incentive to participate in the match. A larger value of  $\gamma$  means more inertia in  $w_t$ : a given shock to  $\vartheta_t$  is associated with a smaller change in  $w_t$ . For simplicity, in this subsection, we abstract from the hiring cost (i.e.,  $\kappa = 0$ ).

We seek to evaluate the generic formula for the steady-state elasticity of labor market tightness with respect to technology (i.e., equation (19)) for the simple wage rule (37). Note that in steady state,  $\frac{dw}{d\vartheta} = \phi$ . Inserting the latter result, together with the steady-state version of equation (37), into equation (19) yields the following expression for the steady-state elasticity:

$$\eta_{\Gamma, \vartheta}^{steady} = \frac{1}{\sigma}.$$

Note that the steady-state elasticity is independent of the fundamental surplus. Moreover, the elasticity is identical to one implied by the Nash bargaining model with  $\eta = D = 0$ .

To derive the actual dynamics of the simple model, we must take a stand on the law of motion for  $\vartheta_t$ . To this end, we assume that

$$\vartheta_t = (1 - v)\vartheta + v\vartheta_{t-1} + \varepsilon_t, \tag{38}$$

where  $\varepsilon_t$  is uncorrelated over time and uncorrelated with  $\vartheta_{t-u}$  for  $u > 0$ .

In Section B of the Technical Appendix we show that the equilibrium solution for the value of a worker to the firm,  $J_t$ , is given by:

$$J_t = \delta_0 + \delta_1 \vartheta_t, \tag{39}$$

where

$$\delta_0 = -\frac{\gamma(1-\phi)\vartheta - \beta\rho\delta_1(1-\nu)\vartheta}{1-\beta\rho} \text{ and } \delta_1 = \frac{(1-\phi)(1+\gamma)}{1-\beta\rho\nu}.$$

Combining the free-entry condition (16) with the solution for  $J_t$ , we obtain

$$\frac{S}{\sigma_m} \Gamma_t^\sigma = J_t = \delta_0 + \delta_1 \vartheta_t.$$

Totally differentiating and rearranging yields the following expression for the dynamic elasticity of labor market tightness with respect to the marginal revenue product:

$$\eta_{\Gamma, \vartheta}^{\text{dynamic}} \equiv \frac{\frac{d\Gamma_t}{\Gamma_t}}{\frac{d\vartheta_t}{\vartheta_t}} = \frac{1}{\sigma} \frac{(1-\phi)(1+\gamma)}{(1-\phi)(1+\gamma) - \frac{1-\beta\rho\nu}{1-\beta\rho} \left( \gamma(1-\phi) - \frac{\beta\rho(1-\phi)(1+\gamma)(1-\nu)}{1-\beta\rho\nu} \right)}. \quad (40)$$

Consider  $\nu$  close to unity, so that the marginal revenue product of a worker is close to a random walk. The limiting case implies that a shock to  $\vartheta_t$  is permanent, which mimics the permanent shift in technology considered in the comparative steady-state analyses in Section 3. For  $\nu \rightarrow 1$ , the dynamic elasticity (equation (40)) becomes

$$\eta_{\Gamma, \vartheta}^{\text{dynamic}} \simeq \frac{1}{\sigma} (1+\gamma) = \eta_{\Gamma, \vartheta}^{\text{steady}} (1+\gamma).$$

Note that if  $\gamma > 0$ , then  $\eta_{\Gamma, \vartheta}^{\text{dynamic}} > \eta_{\Gamma, \vartheta}^{\text{steady}}$ . The restriction on the parameters  $\phi > \gamma(1-\phi)$  discussed above implies that  $\phi > \frac{\gamma}{1+\gamma}$  or  $\gamma < \frac{\phi}{(1-\phi)}$ . By making  $\gamma$  sufficiently large (i.e., by making wages sufficiently inertial),  $\eta_{\Gamma, \vartheta}^{\text{dynamic}}$  can be made arbitrarily large, even though  $\eta_{\Gamma, \vartheta}^{\text{steady}}$  is always simply equal to  $1/\sigma$ . That is, the more inertia there is in wages, the larger is the impact of a shock to  $\vartheta_t$  on labor market tightness and unemployment. Clearly, in this example comparative steady-state analysis is very misleading about the dynamic effects of a persistent shock to technology. Also notice that the parameter  $\gamma$ , which plays a central role in  $\eta_{\Gamma, \vartheta}^{\text{dynamic}}$ , is completely absent from the fundamental surplus formula. So, the latter is not helpful for anticipating the results from a dynamic analysis of a shock to the marginal revenue product of labor.

#### 4.2. Wage inertia in an estimated dynamic search and matching model

In this subsection, we consider the model of CET, who embed the labor market model of Subsection 2 into a medium-sized DSGE NK model.

##### 4.2.1. Households

The economy is populated by a large number of identical households. The representative household has a unit measure of workers, which it supplies inelastically to the labor market. We denote the fraction of employed workers in the representative household in period  $t$  by  $l_t$ . An employed worker earns the nominal wage rate,  $W_t$  and an unemployed worker receives  $D_t$  goods in government-provided unemployment compensation. Each worker has the same concave preferences over consumption. Households provide perfect consumption insurance to their members, so that each worker receives the same level of consumption,  $C_t$ . The preferences of the representative household are the equally weighted average of the preferences of its workers:

$$E_0 \sum_{t=0}^{\infty} \beta^t \ln(C_t - bC_{t-1}), \quad (41)$$

where the parameter  $0 \leq b < 1$  controls the degree of habit formation in preferences. The representative household's budget constraint is

$$P_t C_t + P_{I,t} I_t + B_{t+1} \leq (R_{K,t} u_t^K - a(u_t^K) P_{I,t}) K_t + (1-l_t) P_t D_t + W_t l_t + R_{t-1} B_t - T_t. \quad (42)$$

Here,  $T_t$  denotes lump sum taxes net of profits,  $P_t$  denotes the price of consumption goods,  $P_{I,t}$  denotes the price of investment goods,  $B_{t+1}$  denotes one period risk free bonds purchased in period  $t$  with gross return,  $R_t$  and  $I_t$  denotes the quantity of investment goods. The object  $R_{K,t}$  denotes the rental rate of capital services,  $K_t$  denotes the household's beginning of period  $t$  stock of capital,  $a(u_t^K)$  denotes the cost, in units of investment goods, of the capital utilization rate,  $u_t^K$  and  $u_t^K K_t$  denotes the household's period  $t$  supply of capital services. We discuss details about the capital utilization cost function in Subsection 4.2.4. All prices, taxes and profits in equation (42) are in nominal terms. The representative household's stock of capital evolves as follows:

$$K_{t+1} = (1-\delta_K) K_t + (1-S(I_t/I_{t-1})) I_t,$$

where  $\delta_K$  denotes the depreciation rate and  $S(I_t/I_{t-1})$  are convex investment adjustment costs. We discuss details about the latter in Subsection 4.2.4.

#### 4.2.2. Final goods producers

A final homogeneous good,  $Y_t$ , is produced by competitive and identical firms using the following technology:

$$Y_t = \left( \int_0^1 (Y_{j,t})^{\frac{1}{\lambda}} dj \right)^\lambda, \quad (43)$$

where  $\lambda > 1$ . The representative firm chooses specialized inputs,  $Y_{j,t}$ , to maximize profits:

$$P_t Y_t - \int_0^1 P_{j,t} Y_{j,t} dj,$$

subject to the production function (43). Output,  $Y_t$ , can be used to produce either consumption goods or investment goods. The production of the latter uses a linear technology in which one unit of  $Y_t$  is transformed into  $\Psi_t$  units of  $I_t$ .

#### 4.2.3. Retailers and wholesalers

The  $j^{\text{th}}$  input good in (43) is produced by a retailer, with production function

$$Y_{j,t} = k_{j,t}^\alpha (z_t h_{j,t})^{1-\alpha} - \varphi_t.$$

Here,  $k_{j,t}$  denotes the total amount of capital services purchased by firm  $j$  and  $\varphi_t$  represents a fixed cost of production, which evolves according to an exogenous stochastic process that is consistent with balanced growth. We discuss details about the latter in Subsection 4.2.4. The variable  $z_t$  is a technology shock and  $h_{j,t}$  is the quantity of an intermediate good purchased by the  $j^{\text{th}}$  retailer. This good is purchased in competitive markets at the price  $P_t^h$  from a wholesaler, discussed in Section 2. To produce in period  $t$ , the retailer must borrow  $P_t^h h_{j,t}$  at the gross nominal interest rate,  $R_t$ . The retailer repays the loan at the end of period  $t$  after receiving sales revenues. The  $j^{\text{th}}$  retailer sets its price,  $P_{j,t}$ , subject to the demand curve for its good, and a Calvo sticky price friction. With probability  $1 - \xi$ , the retailer can reoptimize his price, and with probability  $\xi$ ,  $P_{j,t} = P_{j,t-1}$ .<sup>31</sup>

Wholesaler firms produce the intermediate good using labor, which has a fixed marginal productivity of unity. The real price of the intermediate good is  $P_t^h/P_t$  where  $P_t^h$  and  $P_t$  are the nominal prices of the intermediate good and final good, respectively. Let  $\vartheta_t \equiv P_t^h/P_t$ , which is the marginal revenue of wholesalers. Then the analysis of the labor market discussed in Sections 2 and 3 obtains directly with the understanding that all of the shocks to the economy, including monetary policy, affect  $\vartheta_t$ , thereby affecting firms' incentives to post vacancies.

#### 4.2.4. Monetary policy and functional forms

We adopt the following specification for monetary policy:

$$\ln(R_t/R) = \rho_R \ln(R_{t-1}/R) + (1 - \rho_R)[r_\pi \ln(\pi_t/\pi) + r_y \ln(GDP_t/GDP_t^*)] + \sigma_R \varepsilon_{R,t}.$$

Here,  $\pi$  denotes the monetary authority's target inflation rate. The monetary policy shock,  $\varepsilon_{R,t}$ , has unit variance and zero mean. Also,  $R$  is the steady-state value of  $R_t$ . The variable,  $GDP_t$ , denotes gross domestic product (GDP), which equals  $C_t + I_t/\Psi_t + G_t$ . We assume that the growth rate of neutral technological progress,  $\ln \mu_{z,t} \equiv \ln(z_t/z_{t-1})$ , is i.i.d. and that the growth rate of investment-specific technological progress,  $\ln \mu_{\psi,t} \equiv \ln(\Psi_t/\Psi_{t-1})$ , follows a stochastic first-order autoregressive process.

The sources of growth in the model are neutral and investment-specific technological progress because  $\Psi_t$  and  $z_t$  grow over time. Let  $\Phi_t = \Psi_t^{(\alpha/(1-\alpha))} z_t$  denote the composite level of technology. To guarantee balanced growth in the non-stochastic steady state, we require that each element in  $[\varphi_t, s_t, \kappa_t, \gamma_t, G_t, D_t]$  grows at the same rate as  $\Phi_t$  in the steady state. To this end, we adopt the following specification:

$$[\varphi_t, s_t, \kappa_t, \gamma_t, G_t, D_t]' = [\varphi, s, \kappa, \gamma, G, D]' \Omega_t.$$

Here,  $\Omega_t$  is a diagonal matrix with the  $i^{\text{th}}$  diagonal element,  $\Omega_t^i$ , where  $i \in \varphi, s, \kappa, \gamma, G, D$  and  $\Omega_t^i = \Phi_{t-1}^{\theta_i} (\Omega_{t-1}^i)^{1-\theta_i}$ .<sup>32</sup>

The cost of adjusting investment takes the form

$$S(I_t/I_{t-1}) = 0.5(\exp[\sqrt{S''}(I_t/I_{t-1} - \mu \times \mu_\psi)] + \exp[-\sqrt{S''}(I_t/I_{t-1} - \mu \times \mu_\psi)]) - 1.$$

<sup>31</sup> We assume that producers make their price-setting decision before observing the current-period realization of the monetary policy shock but after the time  $t$  technology shocks.

<sup>32</sup> With this specification,  $\Omega_t^i/\Phi_{t-1}$  converges to a constant in the non-stochastic steady state, for each  $i$ . When  $\theta_i$  is close to zero,  $\Omega_t^i$  is virtually unresponsive in the short run to an innovation in either of the two technology shocks, a feature that we find attractive on a priori grounds.

**Table 3**  
Non-estimated parameters and calibrated variables.

| Parameter                           | Value  | Description                              |
|-------------------------------------|--------|--|
| <i>Panel A: Parameters</i>          |        |  |
| $\delta_K$                          | 0.025  | Depreciation rate of physical capital    |
| $\beta$                             | 0.9968 | Discount factor                          |
| $\rho$                              | 0.9    | Job survival probability                 |
| $M$                                 | 60     | Max. bargaining rounds per quarter (AOB) |
| $400\ln(\mu)$                       | 1.7    | Annual output per capita growth rate     |
| $400\ln(\mu \cdot \mu_\psi)$        | 2.9    | Annual investment per capita growth rate |
| <i>Panel B: Steady-State Values</i> |        |  |
| $400(\pi - 1)$                      | 2.5    | Annual net inflation rate                |
| <i>profits</i>                      | 0      | Intermediate goods producers' profits    |
| $Q$                                 | 0.7    | Vacancy-filling rate                     |
| $u$                                 | 0.055  | Unemployment rate                        |
| $G/Y$                               | 0.2    | Government cons. to gross output ratio   |

Notes: Table based on CET.

Here,  $\mu$  and  $\mu_\psi$  denote the unconditional growth rates of  $\Phi_t$  and  $\Psi_t$ . Also,  $S''$  denotes the second derivative of  $S(\cdot)$ , evaluated in the steady state. The cost associated with setting capacity utilization is given by

$$a(u_t^K) = \sigma_a \sigma_b (u_t^K)^2 / 2 + \sigma_b (1 - \sigma_a) u_t^K + \sigma_b (\sigma_a / 2 - 1)$$

where  $\sigma_a$  and  $\sigma_b$  are positive scalars. For a given value of  $\sigma_a$ , we select  $\sigma_b$  so that the steady-state value of  $u_t^K$  is unity.

Finally, we refer the reader to CET and CET's technical appendix for the market clearing conditions, the definition of equilibrium and the set of dynamic and steady-state equilibrium equations.

#### 4.2.5. The role of wage inertia in the estimated model

CET estimate the medium-sized DSGE NK model discussed above for various wage bargaining environments. Their estimation strategy is a Bayesian variant of the strategy in Christiano et al. (2005) that minimizes the distance between the dynamic responses to three shocks in the model and the analog objects in the data. The shocks used by CET include a shock to monetary policy, a neutral technology shock, and an investment-specific technology shock. The dynamic responses to those shocks are obtained using an identified vector autoregression (VAR) for postwar quarterly U.S. time series that includes key labor market variables (see CET for further details).

Here, we focus on the versions of the model in which wages are determined by Nash and AOB bargaining. Table 3 reports the values of parameters that CET set a priori. Table 4 reports the mean and 95 percent probability intervals for the priors and posteriors of the estimated parameters in the Nash and AOB bargaining models. Table 1 reports the implied steady states.

Note that the estimated values of the replacement ratio  $D/w$  in the Nash and AOB models are 0.88 and 0.37, respectively. The estimated value of the replacement ratio, 0.88, in the Nash model is strongly at odds with the micro evidence (see Subsection 3.2). Given that in the Nash model, the posterior mode of  $D/w$  is in the tail of the prior distribution, the marginal likelihood of the Nash model is about 14 log points lower than the AOB model. We also find it useful to consider the restricted Nash model defined in Section 3; that is, we set  $D/w$  to 0.37, keeping all other estimated parameters in the estimated Nash model unchanged.

The solid thin black lines in rows 1 and 2 of Fig. 4 display VAR-based estimates of the dynamic responses of the unemployment rate, the real wage rate and the inflation rate to a monetary policy shock and a neutral technology shock.<sup>33</sup> The grey bands correspond to 95 percent confidence intervals. The blue lines correspond to the dynamic response functions of the Nash model, evaluated at the mode of the parameter estimates. Notice that the model does a good job of matching the dynamic response of unemployment to both shocks. There is no Shimer puzzle here.

This result depends critically on the fact that the model does a reasonably good job of matching the inertial response of real wages to the shocks. To substantiate this claim, we consider the following experiment. We impose on the model the assumption that real wages go up, in period 1, by 50 percent more than their peak response in the estimated Nash model and then stay at that level for three consecutive years. After the three years, the economy returns to the wage rule implied by the restricted Nash-sharing rule. The dot-dashed red lines in Fig. 4 display the implied impulse response functions. The response functions are calculated using the Fair and Taylor (1983) perfect foresight simulation method in which households and firms know, at the time of the shock, the assumed wage path in the experiment, see Christiano et al. (2015) for a detailed description.

The key result here is that for both shocks, the response of unemployment is much smaller, in absolute value, than in the estimated model. For the monetary policy shock, the response is counterfactually small, even taking VAR sampling uncertainty into account: without wage inertia, there is a Shimer-like puzzle. Note also that by construction, the estimated

<sup>33</sup> For brevity and without loss of generality, we exclude the responses to the investment-specific technology shock.

**Table 4**  
Priors and Posteriors of Parameters in Estimated Bargaining Models.

|  | Prior distribution<br>$\mathcal{D}$ , <b>Mode</b> , [2.5-97.5%] | Alternating offer bargaining<br>Posterior distribution<br><b>Mode</b> , [2.5-97.5%] | Nash bargaining           |
|--|---|---|---------------------------|
| <i>Price Setting Parameters</i>              |   |   |                           |
| Price Stickiness, $\xi$                      | $\mathcal{B}$ , <b>0.68</b> , [0.45 0.84]                       | <b>0.75</b> , [0.69 0.78]   | <b>0.74</b> , [0.69 0.79] |
| Price Markup, $\lambda$                      | $\mathcal{G}$ , <b>1.19</b> , [1.11 1.31]                       | <b>1.42</b> , [1.33 1.51]   | <b>1.43</b> , [1.35 1.52] |
| <i>Monetary Authority Parameters</i>         |   |   |                           |
| Taylor Rule: Smooth., $\rho_R$               | $\mathcal{B}$ , <b>0.76</b> , [0.37 0.94]                       | <b>0.84</b> , [0.81 0.87]   | <b>0.84</b> , [0.82 0.87] |
| Taylor Rule: Inflation, $r_\pi$              | $\mathcal{G}$ , <b>1.69</b> , [1.42 2.00]                       | <b>1.38</b> , [1.21 1.65]   | <b>1.38</b> , [1.23 1.69] |
| Taylor Rule: GDP, $r_y$                      | $\mathcal{G}$ , <b>0.08</b> , [0.03 0.22]                       | <b>0.03</b> , [0.01 0.07]   | <b>0.04</b> , [0.02 0.08] |
| <i>Preferences and Technology Parameters</i> |   |   |                           |
| Consumption Habit, $b$                       | $\mathcal{B}$ , <b>0.50</b> , [0.21 0.79]                       | <b>0.80</b> , [0.78 0.84]   | <b>0.81</b> , [0.78 0.84] |
| Cap. Util. Adj. Cost, $\sigma_a$             | $\mathcal{G}$ , <b>0.32</b> , [0.09 1.23]                       | <b>0.11</b> , [0.04 0.30]   | <b>0.18</b> , [0.05 0.32] |
| Investment Adj. Cost, $S''$                  | $\mathcal{G}$ , <b>7.50</b> , [4.57 12.4]                       | <b>15.7</b> , [11.0 19.6]   | <b>15.2</b> , [10.7 19.0] |
| Capital Share, $\alpha$                      | $\mathcal{B}$ , <b>0.33</b> , [0.28 0.38]                       | <b>0.26</b> , [0.20 0.27]   | <b>0.23</b> , [0.21 0.27] |
| Technology Diffusion, $\theta$               | $\mathcal{B}$ , <b>0.50</b> , [0.13 0.87]                       | <b>0.05</b> , [0.02 0.07]   | <b>0.03</b> , [0.01 0.05] |
| <i>Labor Market Parameters</i>               |   |   |                           |
| Prob. Barg. Breakup, $100\delta$             | $\mathcal{G}$ , <b>0.18</b> , [0.04 1.53]                       | <b>0.19</b> , [0.09 0.37]   | -                         |
| Replacement Ratio, $D/w$                     | $\mathcal{B}$ , <b>0.39</b> , [0.21 0.60]                       | <b>0.37</b> , [0.22 0.63]   | <b>0.88</b> , [0.85 0.90] |
| Hiring Cost/Output, $100\eta_h$              | $\mathcal{G}$ , <b>0.91</b> , [0.50 1.67]                       | <b>0.46</b> , [0.24 0.84]   | <b>0.64</b> , [0.34 1.07] |
| Search Cost/Output, $100\eta_s$              | $\mathcal{G}$ , <b>0.05</b> , [0.01 0.28]                       | <b>0.03</b> , [0.00 0.12]   | <b>0.02</b> , [0.00 0.09] |
| Match. Fun. Parameter, $\sigma$              | $\mathcal{B}$ , <b>0.50</b> , [0.31 0.69]                       | <b>0.55</b> , [0.47 0.61]   | <b>0.54</b> , [0.47 0.61] |
| <i>Exogenous Processes Parameters</i>        |   |   |                           |
| Std. Mon. Pol., $400\sigma_R$                | $\mathcal{G}$ , <b>0.65</b> , [0.56 0.75]                       | <b>0.63</b> , [0.57 0.70]   | <b>0.63</b> , [0.58 0.70] |
| Std. Neut. Tech., $100\sigma_{\mu_z}$        | $\mathcal{G}$ , <b>0.08</b> , [0.03 0.22]                       | <b>0.16</b> , [0.11 0.19]   | <b>0.14</b> , [0.11 0.18] |
| Std. Inv. Tech., $100\sigma_\psi$            | $\mathcal{G}$ , <b>0.08</b> , [0.03 0.22]                       | <b>0.12</b> , [0.08 0.15]   | <b>0.11</b> , [0.08 0.16] |
| AR(1) Invest. Tech., $\rho_\psi$             | $\mathcal{B}$ , <b>0.75</b> , [0.53 0.92]                       | <b>0.72</b> , [0.60 0.85]   | <b>0.74</b> , [0.59 0.83] |
| <i>Memo Item</i>                             |   |   |                           |
| Log Marginal Likelihood:                     |   | 286.7   | 272.9                     |

Notes: Posterior mode and parameter distributions are based on a standard MCMC algorithm with a total of 10 million draws (11 chains, 50 percent of draws used for burn-in, draw acceptance rates about 0.24).  $\mathcal{B}$  and  $\mathcal{G}$  denote beta and gamma distributions, respectively. Source: CET.

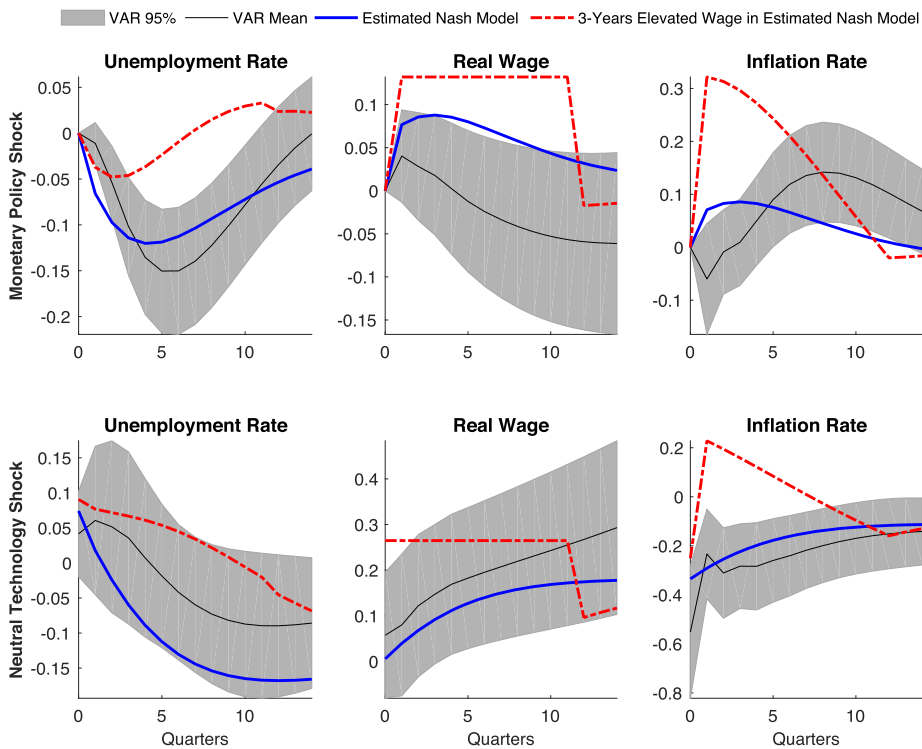
Nash model and the estimated Nash model with three years of elevated wages have the same steady state so the fundamental surplus is exactly the same in both models. So, the fundamental surplus contains no information about the dynamic responses of the two economies being compared.

Rows 1 and 2 of Fig. 5 report the results for the restricted Nash model. From the solid blue lines, we see that real wages respond to both shocks by a counterfactually large amount. Not surprisingly, the response of unemployment in this model is much smaller than in the estimated Nash model. Again, without wage inertia, there is a Shimer-like puzzle. The dot-dashed lines display the impulse response functions if we hold real wages fixed for three consecutive years and then let wages be determined by the Nash-sharing rule afterward. With inertial wages, unemployment now responds by much more. So, wage inertia allows a Nash model with a low replacement ratio to overcome the Shimer-like puzzle. Note again that the two models being compared have identical steady states and fundamental surpluses.

Finally, rows 1 and 2 of Fig. 6 repeat the experiment presented in Fig. 4 for the estimated AOB model. The results are consistent with those emerging from the estimated Nash model. Again, wage inertia plays a pivotal role for the model's ability to account for the dynamic response of unemployment to shocks. And again, the fundamental surplus is fundamentally uninformative about the model's dynamic impulse response functions.

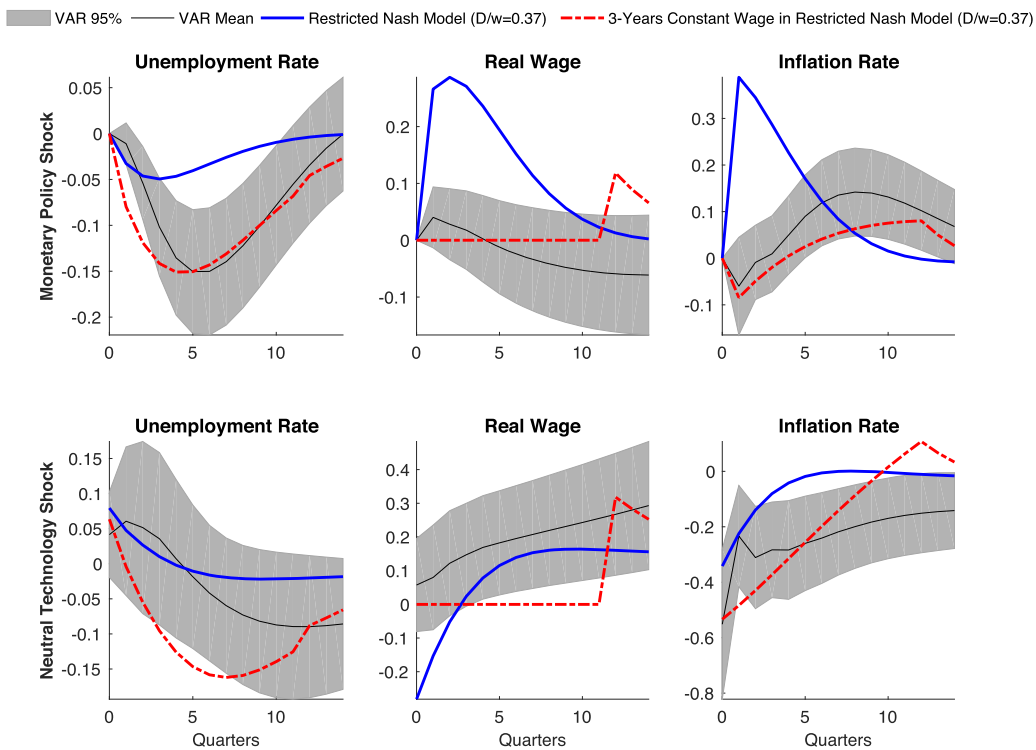
The results in this section highlight the potential danger of using comparative steady-state analyses as a substitute for dynamic analyses. This warning is particularly clear in the case of monetary policy shocks that have no impact on the steady state. Nevertheless, different models of wage determination imply very different responses of unemployment to a monetary policy shock.

As we noted in the introduction, there do exist assumptions under which comparative steady-state analyses do a reasonably good job of mimicking dynamics (i.e., shocks are close to a random walk and there are no important state variables). These assumptions are not satisfied in CET. Another recent example of note is the competitive search model developed in Kehoe et al. (2019), which adopts the specification of preferences developed by Campbell and Cochrane (1999). That specification generates important additional sources of dynamics while leaving no trace in the steady state. A comparative steady-state analysis sheds no light on the interesting dynamic properties of their model.



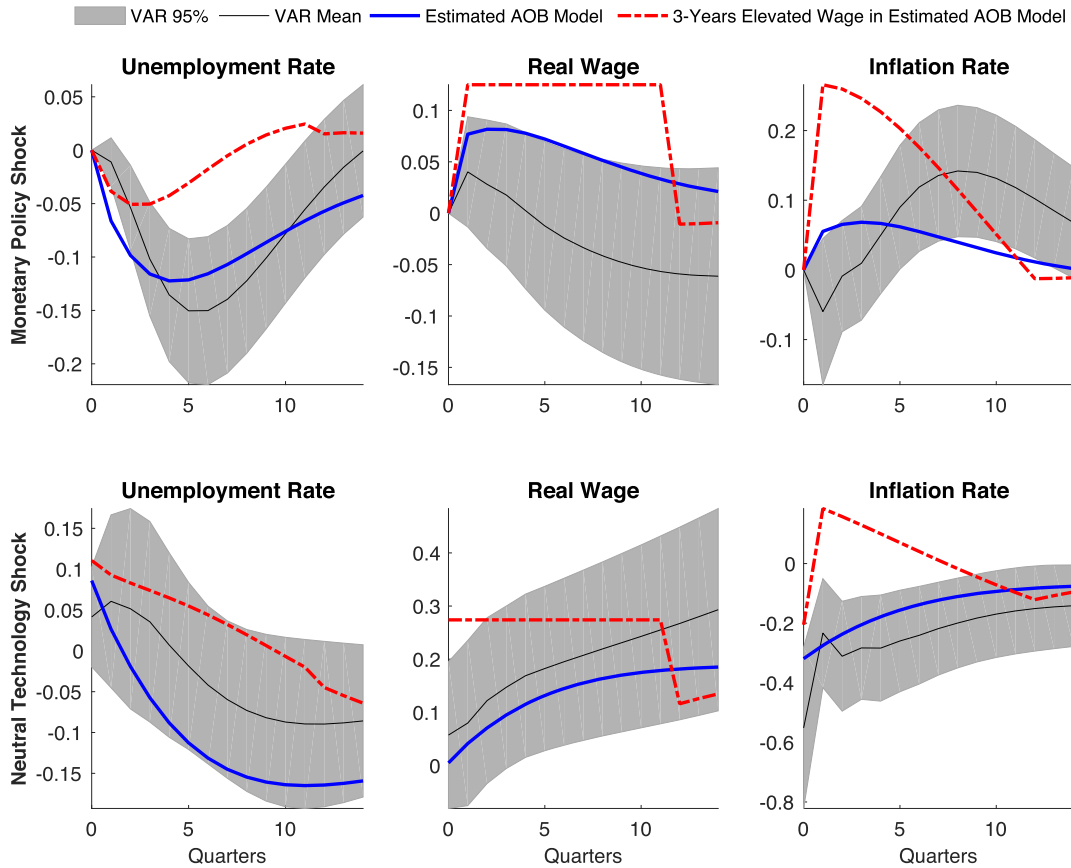
Notes: unemployment in percentage points, real wage in percent deviations and inflation in annualized percentage points.

Fig. 4. Impulse responses in estimated Nash model.



Notes: unemployment in percentage points, real wage in percent deviations and inflation in annualized percentage points.

Fig. 5. Impulse responses in restricted Nash model.



Notes: unemployment in percentage points, real wage in percent deviations and inflation in annualized percentage points.

Fig. 6. Impulse responses in estimated alternating offer bargaining (AOB) model.

### 5. Conclusion

Wage inertia is widely recognized as playing an important role in business cycle fluctuations. An important exception to this view is the search and matching literature where the role of wage inertia is the subject of an ongoing debate. In this paper, we argued that wage inertia does in fact play a crucial role in allowing variants of standard search and matching models to account for the large countercyclical response of unemployment to shocks. We made this argument using comparative steady-state and dynamic analyses of estimated DSGE models. The intuition is straightforward and should not be controversial: if wages increase too much after a change in the marginal revenue product of labor, firms have little incentive to invest in new jobs.

### Technical Appendix

#### Appendix A. Proof of Proposition 1

The set of equilibrium conditions for our AOB model is

$$S^w = w - D + \rho\beta(1 - \sigma_m\Gamma^{1-\sigma})S^w \tag{A.1}$$

$$J = \vartheta - w + \rho\beta J \tag{A.2}$$

$$\frac{s}{\sigma_m}\Gamma^\sigma = J - \kappa \tag{A.3}$$

$$J = \beta_1 S^w - \beta_2 \gamma + \beta_3(\vartheta - D). \tag{A.4}$$

We now derive the two decompositions asserted in Proposition 1.

Adding equations (A.1) and (A.2) and using equation (A.3) to substitute for  $J$ , we reduce the system to two equations:

$$S^w + \frac{s}{\sigma_m} \Gamma^\sigma + \kappa = \vartheta - D + \rho\beta (1 - \sigma_m \Gamma^{1-\sigma}) S^w + \rho\beta \left( \frac{s}{\sigma_m} \Gamma^\sigma + \kappa \right) \quad (\text{A.5})$$

$$\frac{s}{\sigma_m} \Gamma^\sigma + \kappa = \beta_1 S^w - \beta_2 \gamma + \beta_3 (\vartheta - D). \quad (\text{A.6})$$

Using equation (A.6) solve for  $S^w$  in equation (A.5), the system reduces to a single equation in the endogenous variable,  $\Gamma$ :

$$\begin{aligned} & \beta_2 \gamma - \beta_3 (\vartheta - D) + (1 + \beta_1) \left( \frac{s}{\sigma_m} \Gamma^\sigma + \kappa \right) \\ & = \beta_1 (\vartheta - D) + \rho\beta (1 - \sigma_m \Gamma^{1-\sigma}) \left[ \frac{s}{\sigma_m} \Gamma^\sigma + \kappa + \beta_2 \gamma - \beta_3 (\vartheta - D) \right] + \rho\beta_1 \beta \left( \frac{s}{\sigma_m} \Gamma^\sigma + \kappa \right). \end{aligned} \quad (\text{A.7})$$

Totally differentiating with respect to  $\vartheta$  and  $\Gamma$ , using  $f = \sigma_m \Gamma^{1-\sigma}$  and  $Q = \sigma_m \Gamma^{-\sigma}$  in equation (10) and rearranging, we have

$$\frac{\vartheta}{\Gamma} \frac{d\Gamma}{d\vartheta} = \frac{\beta_1 + [1 - \rho\beta(1 - f)]\beta_3}{\left[ (1 + \beta_1)(1 - \rho\beta)\sigma \frac{1}{Q} + \rho\beta\Gamma \right] s + \rho\beta f(\sigma - 1)(\beta_3(\vartheta - D) - \kappa - \beta_2 \gamma)} \vartheta. \quad (\text{A.8})$$

We now turn to the non-structural and structural decompositions of the above expression.

#### A.1. Non-structural decomposition

Solving equation (A.7) for  $s$ :

$$s = \psi \frac{[\beta_1 + \beta_3(1 - \beta\rho(1 - f))](\vartheta - D) - [(1 + \beta_1)(1 - \rho\beta) + \rho\beta f]\kappa - \beta_2(1 - \beta\rho(1 - f))\gamma}{\rho\beta\Gamma + \sigma(1 - \rho\beta)(1 + \beta_1)\frac{1}{Q}}, \quad (\text{A.9})$$

where

$$\psi \equiv \frac{\rho\beta f + \sigma(1 + \beta_1)(1 - \rho\beta)}{\beta\rho f + (1 + \beta_1)(1 - \rho\beta)}.$$

Using equation (A.9) to substitute for  $s$  in the denominator of equation (A.8), that denominator becomes, after collecting terms:

$$\psi a_1 \left[ \vartheta - D - \frac{a_2}{a_1} \kappa - \frac{a_3}{a_1} \gamma \right],$$

where

$$a_1 = \beta_1 + \beta_3 \left[ (1 - \beta\rho(1 - f)) + \frac{\rho\beta f(\sigma - 1)}{\psi} \right]$$

$$a_2 = (1 + \beta_1)(1 - \rho\beta) + \beta\rho f + \frac{\rho\beta f(\sigma - 1)}{\psi}$$

$$a_3 = \left( 1 - \beta\rho(1 - f) + \frac{\rho\beta f(\sigma - 1)}{\psi} \right) \beta_2.$$

Now, we can write equation (A.8) as follows:

$$\frac{\vartheta}{\Gamma} \frac{d\Gamma}{d\vartheta} = \frac{\beta_1 + [1 - \rho\beta(1 - f)]\beta_3}{\psi a_1} \frac{\vartheta}{\vartheta - D - \frac{a_2}{a_1} \kappa - \frac{a_3}{a_1} \gamma},$$

which corresponds to equations (30), (31), (32) and (33), with  $a = a_1$ .

## A.2. Structural decomposition

Factoring  $s/Q$  out of the denominator in equation (A.8), we obtain

$$\frac{\vartheta}{\Gamma} \frac{d\Gamma}{d\vartheta} = \frac{\beta_1 + [1 - \rho\beta(1-f)]\beta_3}{\left[ (1 + \beta_1)(1 - \rho\beta)\sigma + \rho\beta f + \rho\beta f(\sigma - 1)(\beta_3(\vartheta - D) - \kappa - \beta_2\gamma) \frac{Q}{s} \right]} \frac{s}{Q} \vartheta.$$

Rearranging the terms in equation (A.7), we obtain

$$\begin{aligned} \frac{s}{Q} &= \frac{(\beta_1 + (1 - \rho\beta)\beta_3)(\vartheta - D) - (1 + \beta_1)(1 - \rho\beta)\kappa - (1 - \rho\beta)\beta_2\gamma}{(1 + \beta_1)(1 - \rho\beta) + \rho\beta f \left[ 1 + (\kappa + \gamma\beta_2 - \beta_3(\vartheta - D)) \frac{Q}{s} \right]} \\ &= (\beta_1 + (1 - \rho\beta)\beta_3) \frac{\vartheta - D - \tau_\kappa^S \kappa - \tau_\gamma^S \gamma}{(1 + \beta_1)(1 - \rho\beta) + \rho\beta f \left[ 1 + (\kappa + \gamma\beta_2 - \beta_3(\vartheta - D)) \frac{Q}{s} \right]}, \end{aligned}$$

where  $\tau_\kappa^S$  and  $\tau_\gamma^S$  are as defined in equation (29). It then follows that

$$\frac{\vartheta}{\Gamma} \frac{d\Gamma}{d\vartheta} = \frac{\beta_1 + [1 - \rho\beta(1-f)]\beta_3}{\beta_1 + (1 - \rho\beta)\beta_3} \Xi \frac{\vartheta}{\vartheta - D - \tau_\kappa^S \kappa - \tau_\gamma^S \gamma}.$$

Here,

$$\Xi = \frac{(1 + \beta_1)(1 - \rho\beta) + \rho\beta f \left[ 1 + (\kappa + \gamma\beta_2 - \beta_3(\vartheta - D)) \frac{Q}{s} \right]}{(1 + \beta_1)(1 - \rho\beta)\sigma + \rho\beta f \left[ 1 + (\sigma - 1)(\beta_3(\vartheta - D) - \kappa - \beta_2\gamma) \frac{Q}{s} \right]},$$

consistent with the result in equation (28). This establishes Proposition 1.

## Appendix B. Dynamic elasticity formula in inertial wage rule

Here, we derive the equilibrium solution for the value of a worker to a firm,  $J_t$ , provided in Subsection 4.1.

Note that the value of a worker to a firm is given by

$$J_t = \vartheta_t - w_t + \beta\rho E_t J_{t+1}. \quad (\text{B.1})$$

Substituting for  $w_t$  using (37) gives

$$J_t = \vartheta_t - \phi\vartheta_t + \gamma(1 - \phi)(\vartheta_t - \vartheta) + \beta\rho E_t J_{t+1}. \quad (\text{B.2})$$

Next, we solve for  $J_t$  using the method of undetermined coefficients. We guess that the solution takes the following form

$$J_t = \delta_0 + \delta_1 \vartheta_t, \quad (\text{B.3})$$

where  $\delta_0$  and  $\delta_1$  are undetermined coefficients that are to be determined as a function of the model parameters. Substituting (B.3) into (B.2) and making use of (38), we obtain

$$0 = [(1 - \phi)(1 + \gamma) - \delta_1 + \beta\rho\delta_1 v] \vartheta_t + [\beta\rho\delta_0 - \gamma(1 - \phi)\vartheta - \delta_0 + \beta\rho\delta_1(1 - v)\vartheta].$$

Setting the terms in the two square brackets to zero and solving for  $\delta_0$  and  $\delta_1$ , gives

$$\delta_0 = -\frac{\gamma(1 - \phi)\vartheta - \beta\rho\delta_1(1 - v)\vartheta}{1 - \beta\rho} \text{ and } \delta_1 = \frac{(1 - \phi)(1 + \gamma)}{1 - \beta\rho v}.$$

Next, combining the free-entry condition (16) with the solution for  $J_t$  gives

$$\frac{s}{\sigma_m} \Gamma_t^\sigma = J_t = \delta_0 + \delta_1 \vartheta_t.$$

Totally differentiating:

$$\frac{s}{\sigma_m} \sigma \Gamma^\sigma \frac{d\Gamma_t}{\Gamma} = \delta_1 \vartheta \frac{d\vartheta_t}{\vartheta}.$$

Rearranging and using  $\frac{s}{\sigma_m} \Gamma^\sigma = \delta_0 + \delta_1 \vartheta$  yields

$$\begin{aligned} \eta_{\Gamma, \vartheta}^{dynamic} &\equiv \frac{\frac{d\Gamma_t}{\Gamma}}{\frac{d\vartheta_t}{\vartheta}} = \frac{\delta_1 \vartheta}{\sigma \frac{s}{\sigma_m} \Gamma^\sigma} \\ &= \frac{1}{\sigma} \frac{(1 - \phi)(1 + \gamma)}{(1 - \phi)(1 + \gamma) - \frac{1 - \beta \rho \nu}{1 - \beta \rho} \left( \gamma(1 - \phi) - \frac{\beta \rho(1 - \phi)(1 + \gamma)(1 - \nu)}{1 - \beta \rho \nu} \right)} \end{aligned}$$

which is the expression for the dynamic elasticity of labor market tightness with respect to the marginal revenue product (or technology) provided in Subsection 4.1.

### Appendix C. Computational experiments associated with the principal components approach

#### C.1. Principal components approach: Nash model with $\kappa > 0$

The elements of the structural decomposition for the Nash model with  $\kappa > 0$  are, after using equation (15) to simplify the terms in (27)–(29),

$$\Upsilon^S = \frac{(1 - \rho\beta) + \eta\rho\beta f \left( 1 + \frac{\kappa}{s} \sigma_m^{\frac{1}{1-\sigma}} (f)^{\frac{-\sigma}{1-\sigma}} \right)}{\sigma(1 - \rho\beta) + \eta\rho\beta f \left( 1 + (1 - \sigma) \frac{\kappa}{s} \sigma_m^{\frac{1}{1-\sigma}} (f)^{\frac{-\sigma}{1-\sigma}} \right)}, \quad \tau_\kappa^S = \frac{1 - \rho\beta}{1 - \eta}. \tag{C.1}$$

The Nash model with  $\kappa > 0$  is also considered by LS and the characterization of the two-factor decomposition of  $\eta_{\Gamma, \vartheta}$  that they work with corresponds to equation (C.1).<sup>34</sup> The numerator term for  $\tau_\kappa^S$  in equation (C.1),  $1 - \rho\beta$ , converts  $\kappa$  into an annuity value. LS claim that their intuitive definition of the FS naturally implies that  $1 - \rho\beta$  should be amplified by dividing by  $1 - \eta$ . LS do not consider the second of the two-factor decompositions of  $\eta_{\Gamma, \vartheta}$  implied by Proposition 1: the non-structural decomposition. That decomposition is, after using equation (15) to rearrange the terms in (30)–(33), given by

$$\Upsilon^{NS} = \frac{\eta\rho\beta f + (1 - \rho\beta)}{\eta\rho\beta f + \sigma(1 - \rho\beta)}, \quad \tau_\kappa^{NS} = \tau_\kappa^S + \frac{\eta}{1 - \eta} \beta \rho f \left[ 1 + (\sigma - 1) \Upsilon^{NS} \right]. \tag{C.2}$$

Evidently,  $\tau_\kappa^{NS}$  could be very different from  $\tau_\kappa^S$ .

To apply the principal components approach, we adopt the following measure,  $\nu$ , of the role of the inverse FS in transmitting the effect of a change in a model parameter into a change in the tightness elasticity,  $\eta_{\Gamma, \vartheta}$ :

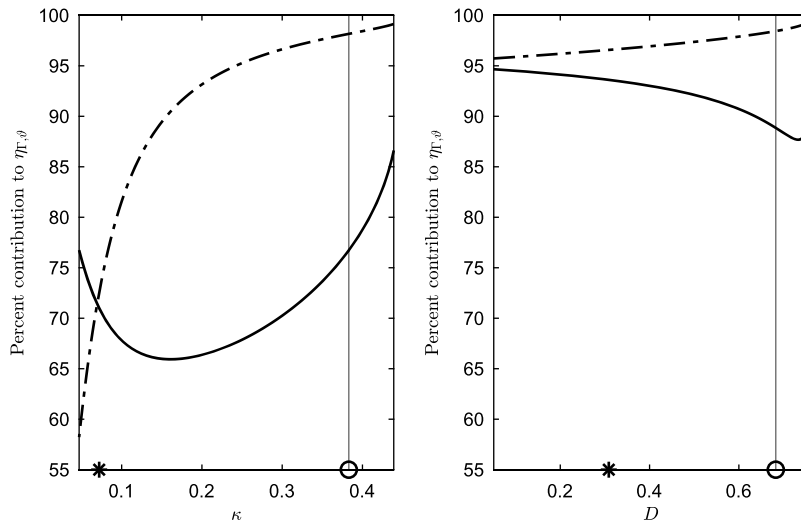
$$\nu = 100 \frac{\log(1/FS) - \log(1/\hat{FS})}{\log(\eta_{\Gamma, \vartheta}) - \log(\hat{\eta}_{\Gamma, \vartheta})}. \tag{C.3}$$

Here, the hat over  $\eta_{\Gamma, \vartheta}$  and  $1/FS$  indicates that those objects are evaluated at a set of baseline parameter values. The variables without a hat are evaluated at a point in which one parameter is perturbed from its baseline value. Let  $\nu^S$  and  $\nu^{NS}$  denote the values of  $\nu$  when FS is constructed using the structural and non-structural decompositions in Proposition 1, respectively. We compute  $\nu^S$  and  $\nu^{NS}$  on a grid of admissible values of  $\kappa$ ,  $\kappa \in [0, \bar{\kappa}]$ , where  $\bar{\kappa}$  is the value of  $\kappa$  for which  $f$  is close to zero when all other parameters (including  $D$ ) are held at their estimated values. We constructed the analogous set of admissible values for  $D$ .

The baseline parameters used in Fig. 7 are the ones reported for the Nash model in Table 1. The left panel in Fig. 7 displays the graph of  $\nu^S$  and  $\nu^{NS}$  for the admissible values of  $\kappa$ , and the right panel reports results for the admissible values of  $D$ . The asterisk in each panel of Fig. 7 indicates the baseline value of the indicated parameter. Equation (C.3) is not defined at the asterisk point, and so this point was excluded from the grid of values of  $\kappa$  and  $D$  considered. The vertical lines in each panel of the figure indicate the value of the variable on the horizontal axis, which, conditional on the other variables taking on their values, generates a value of 24.92 for the market tightness elasticity,  $\eta_{\Gamma, \vartheta}$ .

Consider the right panel of Fig. 7. Evidently, the LS narrative holds up well for both the structural (dot-dashed line) and the non-structural (solid line) decompositions. Over 90 percent of the impact of any admissible perturbation in  $D$  on  $\eta_{\Gamma, \vartheta}$  operates through the inverse FS. The LS narrative does somewhat better under the structural decomposition in that  $\nu^S$  is always closer to 100 percent. The vertical line indicates that raising the tightness elasticity to 24.92 by increasing  $D$

<sup>34</sup> This model is studied in section A.5 of the Online Technical Appendix to LS. See their equation (86) for  $\tau_\kappa^S$ , and equation (74) for  $\Upsilon^S$ .



Note: Dash-dot line and solid lines correspond to structural and non-structural decompositions, respectively. Parameter values reported in Table 1 are indicated by \*. The objects graphed are  $\nu^S$  and  $\nu^{NS}$ , defined in equation (C.3). The  $\alpha$  variables in equation (C.3) are evaluated at the Table 1 values of the parameters. The estimated values are not included in the grid of values of  $\kappa$  and  $D$  used in the calculations because  $\nu^S$  and  $\nu^{NS}$  are not defined at those points. For  $\kappa = 0.439$ ,  $f = .0023$  and for  $\kappa = 0.047$ ,  $f = 0.9857$ . For  $D = 0.051$ ,  $f = 0.9758$  and for  $D = 0.7557$ ,  $f = 0.004$ . As the values of  $D$  are varied, all other model parameter values (including  $\kappa$ ) are held constant. Similarly, for  $\kappa$ . Circles indicate the values of  $\kappa$  or  $D$  which would set  $\eta_{\Gamma,\vartheta} = 24.2$  without changing any other baseline parameter. In the case of  $\kappa$ , the circle corresponds to  $\kappa = 0.383$  and the value of equation (C.3) is 98.2 percent and 76.7 percent for the structural and non-structural decompositions, respectively. In the case of  $D$ , the circle corresponds to  $D = 0.683$  and the value of equation (C.3) is 98.4 percent and 88.8 percent for the structural and non-structural decompositions, respectively.

Fig. 7. Contribution of inverse FS to  $\eta_{\Gamma,\vartheta}$  in restricted Nash model.

alone requires  $D = 0.683$ . The figure indicates that the rise in the tightness elasticity over its baseline value of 3.97 operates 98.4 percent or 88.8 percent through the inverse FS, depending on which of the two ways of computing FS implied by Proposition 1 is used. Evidently, the two measures of FS are roughly in agreement that the lion's share of the jump in  $\eta_{\Gamma,\vartheta}$  is accomplished through the FS, consistent with the LS narrative.

Turning to the left panel in Fig. 7, we see that the inverse FS channel is bigger than the  $\Upsilon$  channel in transmitting a perturbation in  $\kappa$  to a change in  $\eta_{\Gamma,\vartheta}$ , for all values of  $\kappa$  displayed, because  $\nu^{NS}, \nu^S > 50$ . Over most of the admissible values of  $\kappa$ , the FS channel in the structural decomposition is noticeably larger than it is in the non-structural decomposition. But the relationship flips for small values of  $\kappa$  where the inverse FS in the non-structural decomposition plays a larger role than the inverse FS in the structural decomposition. The region of low values of  $\kappa$  is of some interest because it contains the estimated value of  $\kappa$ . For  $\kappa$  near zero, the inverse FS in the structural decomposition accounts for 60 percent of the effect of  $\kappa$  on  $\eta_{\Gamma,\vartheta}$ , so that  $\Upsilon$  accounts for a hefty 40 percent.

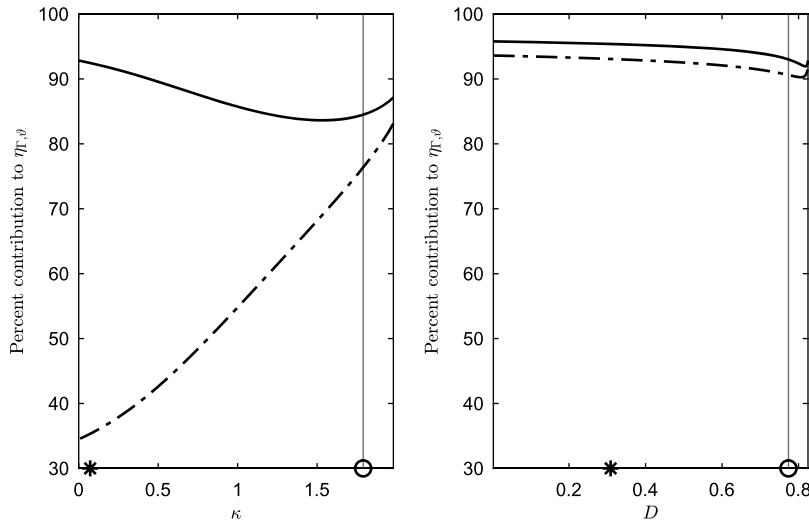
The main takeaway of Fig. 7 is that the LS narrative receives support under both decompositions for all admissible values of  $\kappa$  and  $D$ . For most (but not all) of the perturbations considered, the principal components method finds that the LS in the structural decomposition dominates the LS in the non-structural decomposition. By this metric, LS (see their Online Appendix, equation (86)) choose the “right” measure of the FS for the Nash model with  $\kappa > 0$  when they use the structural decomposition.

The degree of bargaining power in the Nash model with  $\kappa > 0$  just studied is relatively high. So, we also considered the case  $\eta = 0.60$ , and we adjusted the value of  $\sigma_m$  so that  $f$  remains at its value in Table 1. We constructed the analog of Fig. 7 for this alternative baseline parameterization. The results are displayed in Fig. 8. In the case of  $D$  (right panel), it is still true that both decompositions consistently favor the LS narrative, though now the non-structural decomposition dominates the structural decomposition for all admissible values of  $D$ .

The results for  $\kappa$  in the left panel of Fig. 8 are noticeably different from what they were for the higher value of  $\eta$  (see left panel of Fig. 7). Not only is the ranking of the structural and non-structural inverse FS reversed with the lower value of  $\eta$ , but the structural decomposition actually assigns a higher role to  $\Upsilon$  for values of  $\kappa$  less than unity.

Still, under both decompositions, it is the case that the inverse FS plays the lion's share of the role if we are to obtain a sufficiently large jump in the tightness elasticity to get it from its value of 1.94 in the alternative baseline parameterization to 24.92 by increasing  $\kappa$ . In this sense, the results provide some support for the LS narrative. The principal components method suggests that the two-factor decomposition suggested by LS for the Nash model for  $\kappa > 0$  is the “right” one for  $\eta$  high and the “wrong” one for  $\eta$  low. That the principal components approach evidently does not consistently select one of the two measures of FS implied by Proposition 1.

We take away two conclusions from the analysis of the Nash model:



Note: Dot-dashed and solid lines correspond to structural and non-structural decompositions, respectively. Baseline parameterization: same as in restricted Nash column of Table 1, except  $\eta = 0.6$ ,  $\sigma_m = 0.0586$ , with the latter set so that steady state equilibrium  $f = 0.6321$ , its value in Table 1. The value of  $\eta_{\Gamma,\vartheta}$  for this baseline parameterization is 1.94. The baseline parameterization is indicated by the \*. The objects graphed,  $v^S$  and  $v^{NS}$ , are defined in equation (C.3), where variables with a '^' are evaluated at the baseline parameter values. For  $D = 0.001$ ,  $f = 0.8112$  and for  $D = 0.8246$ ,  $f = 0.007$ . For  $\kappa = 1.99$ ,  $f = 0.009$  and for  $\kappa = 0$ ,  $f = 0.6863$ . As the different values of  $\kappa$  are evaluated, other model parameters (including  $D$ ) are held fixed at their baseline values. Similarly for  $D$ . Circles indicate the values of  $\kappa$  or  $D$  which would set  $\eta_{\Gamma,\vartheta} = 24.2$  without changing the value of any other baseline parameter. In the case of  $\kappa$ , the circle corresponds to  $\kappa = 1.79$  and the value of equation (C.3) is 76.4 percent and 84.5 percent for the structural and non-structural decompositions, respectively. In the case of  $D$ , the circle corresponds to  $D = 0.774$  and the value of equation (C.3) is 90.6 percent and 93.0 percent for the structural and non-structural decompositions, respectively.

Fig. 8. Contribution of inverse FS to  $\eta_{\Gamma,\vartheta}$  in Nash model with fixed hiring cost and lower worker bargaining power.

**Fact 1.** Applying the principal components method to the Nash model, we obtain the following results: (1) for all parameter values considered, each of the two-factor decompositions implied by Proposition 1 agrees that raising  $\eta_{\Gamma,\vartheta}$  from its low (less than 4) value in the baseline parameterization to 24.2 requires increasing the inverse FS; and (2) the principal components method designates the structural measure of the FS as the right one for the high value of  $\eta$  and the non-structural measure as the right one for the low value of  $\eta$ . So, the implication of Proposition 1 that the specific value of FS is not well-defined is not resolved by the principal components method.

C.2. Principal components approach: AOB model

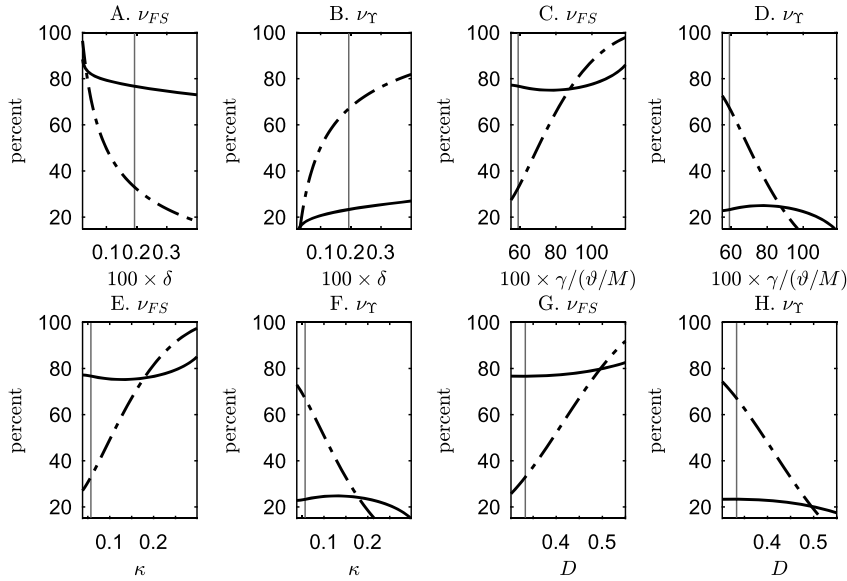
The exercises we now perform for the AOB model are similar to what we do for the Nash model. However, they are adjusted to reflect that our primary interest lies with understanding why the AOB model exhibits so much more labor market volatility than the Nash model. The two two-factor decompositions implied by Proposition 1 in effect give us four factors that can in principle account for the fact that  $\eta_{\Gamma,\vartheta}$  is so much higher in the AOB model than it is in the restricted Nash model (see Table 2). We begin with the estimated AOB model. As noted above, that model implies that a large share of job surplus is transferred to workers. So, afterward we also consider an alternative version of the AOB model in which the share is smaller.

C.2.1. Estimated AOB model

Fig. 9 graphs  $v_{FS}$  and  $v_{\gamma}$  in equation (35) for each decomposition, for all admissible values of the parameters  $\delta$ ,  $\gamma$ ,  $D$  and  $\kappa$ .<sup>35</sup> Each panel indicates the value of  $v_{FS}$  or  $v_{\gamma}$  when the AOB model parameter on the horizontal axis takes on the indicated value and all other parameters of the AOB model are set to their estimated value in Table 2. The solid lines correspond to  $v_{FS}$  or  $v_{\gamma}$  based on the non-structural decomposition and the dot-dashed lines correspond to the structural decomposition. The vertical line in each panel indicates the estimated value in Table 2 of the indicated AOB model parameter. According to equation (35), the statistics  $v_{FS}$  and  $v_{\gamma}$ , require not only the components of the decomposition of  $\eta_{\Gamma,\vartheta}$  in the AOB model but also the components of the decomposition in the estimated restricted Nash model. For the latter, we always evaluate the decomposition at the estimated parameter values of the restricted Nash model reported in Table 2.

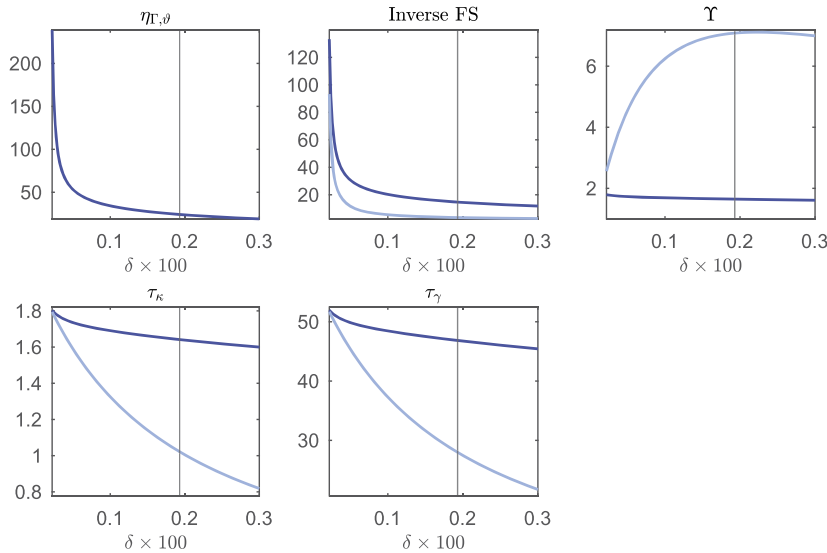
In Fig. 9 we can see the key result reported in Table 2: for the estimated values of  $\delta, \gamma, \kappa, D$ , the higher value of  $\eta_{\Gamma,\vartheta}$  in the AOB model can be accounted for as reflecting a higher inverse FS in the non-structural decomposition (e.g., the

<sup>35</sup> As before, these parameters are 'admissible' as long as they are non-negative and imply  $f \in (0, 1)$ .



Notes: These figures graph  $\nu_{FS}$  and  $\nu_{\Gamma}$  in equation (35) over a grid of admissible values of the parameter indicated on the horizontal axis of each panel. For any parameter, the admissible values are the ones which satisfy non-negativity and  $f \in (0, 1)$ , holding the other AOB model parameter values fixed at their values reported in Table 1 (the solid vertical line in each panel indicate the Table 1 value of the corresponding parameter). The parameter values for the Nash model correspond to the Nash model parameters reported Table 1. The solid line corresponds to the non-structural decomposition and the dot-dashed line corresponds to the structural decomposition. The points of intersection of the vertical line with the dot-dashed and solid lines coincide across all panels for  $\nu_{FS}$ . Similarly for the panels displaying  $\nu_{\Gamma}$ .

Fig. 9. Analysis of factors that account for the rise in  $\eta_{\Gamma, \phi}$  from estimated restricted Nash to estimated AOB models.



Note: See Fig. 1. The lowest value of  $\delta$ ,  $\delta = 0.0002$  corresponds to  $f = 0.02$  and the highest value of  $\delta$ ,  $\delta = 0.003$  corresponds to  $f = 0.84$ .

Fig. 10. Decomposition,  $\delta$  in AOB model.

intersection of the vertical line with the solid line in panels corresponding to  $\nu_{FS}$ ) or a higher value of  $\gamma$  in the structural decomposition (e.g., the intersection of the vertical line with the dot-dashed line in panels corresponding to  $\nu_{\Gamma}$ ).

Taking the principal components perspective, we now examine how well each of the four factors accounts for the higher  $\eta_{\Gamma, \phi}$  in the AOB model across a range of parameter values for the AOB model. The key result is that no one factor is consistently best for all parameter perturbations. For example, Panels A and B indicate that for values of  $\delta$  in the middle and left-of-middle ranges, the inverse FS in the non-structural decomposition is closest to 100 (solid line, Panel A). For higher values of  $\delta$ ,  $\gamma$  in the structural decomposition is closest to 100 (dot-dashed line, Panel B). Now consider  $\gamma$  in Panels C and D. This parameter favors the inverse FS. But for smaller values of  $\gamma$ , the inverse FS in the non-structural decomposition is closest to 100 (solid line) and for higher values of  $\gamma$ , the structural decomposition is closest to 100 (dot-dashed line).

**Table 5**  
Principal component statistic, estimated AOB model.

|                                 | $\delta$ | $\gamma$ | $\kappa$ | $D$   |
|---------------------------------|----------|----------|----------|-------|
| A. Non-structural Decomposition |          |          |          |       |
| $v_{FS}^{NS}$                   | 23.22    | 22.79    | 22.77    | 21.78 |
| $v_{\Upsilon}^{NS}$             | 77.05    | 77.42    | 77.40    | 78.31 |
| B. Structural Decomposition     |          |          |          |       |
| $v_{FS}^S$                      | 65.36    | 37.22    | 37.98    | 45.23 |
| $v_{\Upsilon}^S$                | 41.50    | 73.16    | 72.17    | 62.89 |

Note:  $v_{FS}$  and  $v_{\Upsilon}$  are defined in equation (35) and the superscript *NS* and *S* refer to the non-structural and structural decompositions, respectively. For each parameter indicated in the column header, a grid of admissible values for that parameter was constructed (see text for details). At each grid point the four factors,  $v_{FS}^S$ ,  $v_{\Upsilon}^S$ ,  $v_{FS}^{NS}$ ,  $v_{\Upsilon}^{NS}$  are computed (see the graphs in Fig. 9). The ‘best’ (‘principal’) factor is the one that is closest to 100 at each grid point. A measure of the quality of a factor is its average ‘Error’ across the grid points: the square root of the mean square deviation from 100 of that factor across all grid points. Consider, for example, 23.22 at the top of the column corresponding to  $\delta$ . That is

$Error = \sqrt{\frac{1}{N} \sum_{i=1}^N [100 - v_{FS,i}^{NS}]^2} = 23.19$ , after rounding, where  $N$  is the number of equally-spaced grid points used for  $\delta$ , and  $v_{FS,i}^{NS}$  is the value of  $v_{FS}^{NS}$  at the  $i^{th}$  grid point. The other *Error*’s in the table are constructed in an analogous way.

The results for  $\kappa$  are similar to those for  $\gamma$ . The results for  $D$  deviate somewhat from the pattern set by  $\gamma$  and  $\kappa$ . Panels G and H indicate that, apart from a small region of high values of  $D$ , the inverse FS in the non-structural decomposition is the factor that consistently dominates (solid line, Panel G).

We consider a scalar *principal components statistic* that summarizes how well a particular factor accounts for the impact on  $\eta_{\Gamma,\vartheta}$  of the whole range of perturbations in a particular parameter. The statistic, based on the mean square deviation of the factor from 100, rewards being close to 100, and applies a large penalty to being far from 100. In this way, this measure offers a different perspective from the one we took in examining Fig. 9, where we simply identify which factor is closest to 100 and do not pay attention to how badly a factor does when it is not the best one. Each column in Table 5 corresponds to one of  $\delta$ ,  $\gamma$ ,  $\kappa$ ,  $D$ , and the four numbers provide the principal components statistic for each of the four factors (see the table note for the precise measure). In the case of each parameter, the smallest value of the principal components statistic was achieved by the inverse FS in the non-structural decomposition (see the entries in Fig. 9). So, by this measure, the inverse FS in the non-structural decomposition consistently does best across  $\delta$ ,  $\gamma$ ,  $\kappa$ ,  $D$ .

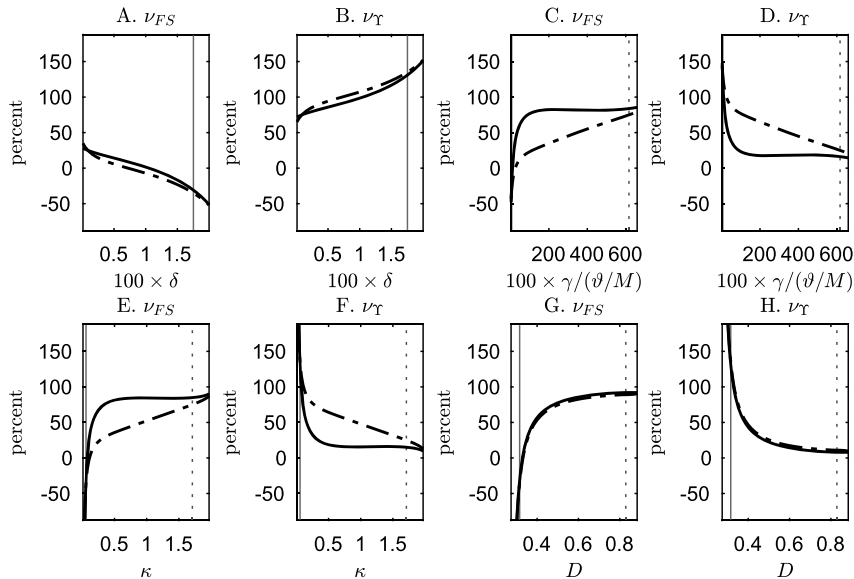
We dig deeper into the previous results for the AOB model by examining Figs. 10, 2, 1 and 3. They display the elements of the two decompositions of  $\eta_{\Gamma,\vartheta}$  for a range of values of  $\delta, \gamma, \kappa$  and  $D$ , respectively.<sup>36</sup> Note that labor market volatility,  $\eta_{\Gamma,\vartheta}$ , displays a pronounced U-shaped pattern as we vary  $\gamma$  and  $D$  (see Figs. 2 and 3). That pattern also appears in the inverse FS in the non-structural decomposition. It may at first seem surprising that  $\eta_{\Gamma,\vartheta}$  could be decreasing in  $\gamma$  or  $D$  in any region. But the reason is that  $\tau_{\gamma}$  and  $\tau_{\kappa}$  are decreasing in  $\gamma$  and  $D$  in the non-structural decomposition and, other things the same, this drives down the inverse FS in that decomposition (see the 2,1 and 2,2 panels in Figs. 2 and 3). Also, note that  $\Upsilon$  remains just below 2 in the non-structural decomposition, essentially requiring that the inverse FS in that decomposition account for most of the variation in  $\eta_{\Gamma,\vartheta}$  (see the 1,3 panels in Figs. 10, 2, 1 and 3). Overall, these observations help to explain the results in Table 5 which indicate that the inverse FS in the non-structural decomposition is the single best factor across the four different candidates.

### C.2.2. Modified version of AOB model with lower share of surplus going to workers

Our estimated AOB model implies that the share of surplus going to workers is high (see Table 1). The principal components method applied to that model supports the LS narrative about the inverse FS in the non-structural decomposition. In this section, we investigate the robustness of that conclusion to a change in the model that reduces the share of surplus going to workers.

We redo the computations in Fig. 9 for an alternative baseline parameterization of the AOB and restricted Nash models, in which 60 percent of total surplus goes to workers. We refer to this baseline parameterization as the *low worker share AOB model*. In this model,  $\delta = 0.0175$  and  $\gamma = 0.0008$ . The latter implies that it costs the firm 5.3 percent of a day’s production by one worker for a firm to prepare a counteroffer. As in the original baseline,  $D$  is set so that  $D/w = 0.37$ . The cost of posting a vacancy,  $s$ , is set to 0.333 to ensure that  $f$  is the same as is the estimated Nash and AOB models in Table 1. For simplicity, we refer to the low  $\eta$  parameterization of the Nash model as the *low worker share Nash model*.

<sup>36</sup> As in Fig. 9, these are one-at-a-time variations in the indicated parameters, holding all other parameters in the model fixed at their estimated values.



Notes: with two exceptions, these figures are constructed as described in the note to Fig. 9. The two exceptions are: (i) the Table 1 parameter values are replaced by the low worker share parameter values for the Nash and AOB models described in the text; and (ii) the vertical dotted line indicates the value of the corresponding parameter which results in  $\eta_{\Gamma,\vartheta} = 24.2$  for the AOB model.

Fig. 11. Analysis of factors that account for the rise in  $\eta_{\Gamma,\vartheta}$  from the Nash to the AOB models, in the low worker share version of these models.

**Table 6**  
Principal component statistic, low worker share AOB model.

|                                 | $\delta$ | $\gamma$ | $\kappa$ | $D$    |
|---------------------------------|----------|----------|----------|--------|
| A. Non-structural Decomposition |          |          |          |        |
| $\nu_{FS}^{NS}$                 | 104.78   | 28.09    | 56.93    | 132.09 |
| $\nu_{\Gamma}^{NS}$             | 20.76    | 78.95    | 87.11    | 132.15 |
| B. Structural Decomposition     |          |          |          |        |
| $\nu_{FS}^S$                    | 110.79   | 58.80    | 65.71    | 134.62 |
| $\nu_{\Gamma}^S$                | 22.10    | 51.11    | 59.13    | 132.13 |

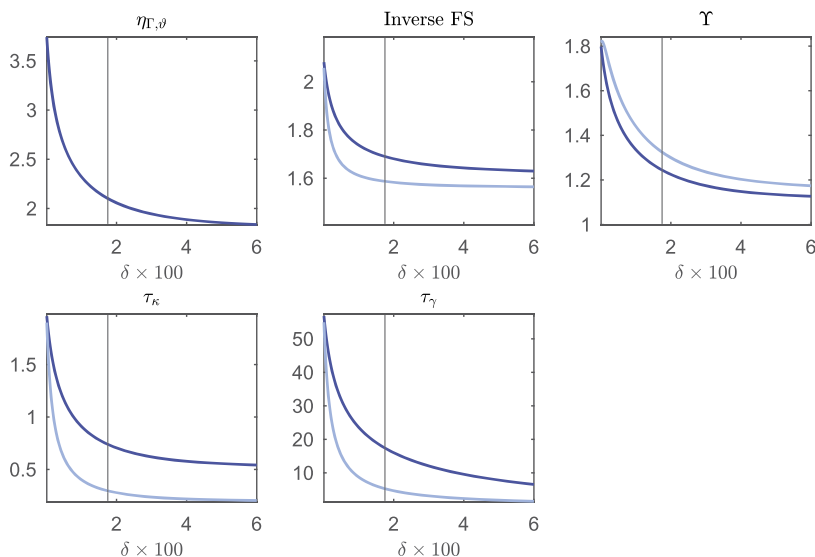
Note: Constructed as explained in note to Table 5, except that the calculations are based on the low worker an alternative baseline set of parameters for the Nash and AOB models. As explained in the text, the alternative baseline is a set of parameters for which the Nash and AOB models both imply that the share of total surplus going to workers is 60 percent. In both models, the finding rate,  $f$ , in the baseline and alternative baseline coincide.

We now report the same set of graphs used above to analyze the low worker share baseline parameterization of the AOB and restricted Nash models. As before, each graph has a vertical solid line which identifies the baseline parameterization. In the low worker share baseline parameterization,  $\eta_{\Gamma,\vartheta} = 2.1$ .<sup>37</sup> With one exception, a vertical dotted line indicates the value of the parameter on the horizontal axis required to obtain  $\eta_{\Gamma,\vartheta} = 24.2$ . The exception is the parameter,  $\delta$ , which cannot produce a high value of  $\eta_{\Gamma,\vartheta}$  when the other parameters are at their low worker share baseline.

According to the results in Panels A and B of Fig. 11, the impact of  $\delta$  on  $\eta_{\Gamma,\vartheta}$  operates primarily through  $\Upsilon$ , and the effect is roughly the same across the two decompositions. This is consistent with the principal component statistics reported for  $\delta$  in Table 6. At the same time, the magnitude of the impact of  $\delta$  on  $\eta_{\Gamma,\vartheta}$  is essentially negligible, with  $\eta_{\Gamma,\vartheta} = 3.8$  when  $\delta = 0$  and  $\eta_{\Gamma,\vartheta} = 2.1$  when  $\delta = 0.02$ . The panels for  $\gamma$  and  $\kappa$  indicate that the inverse FS in the non-structural decomposition works best for those parameters.<sup>38</sup> This is also consistent with the results in the  $\gamma$  and  $\kappa$  columns in Table 6. Finally, in the case of  $D$  the inverse FS in the structural and non-structural decompositions perform about the same.

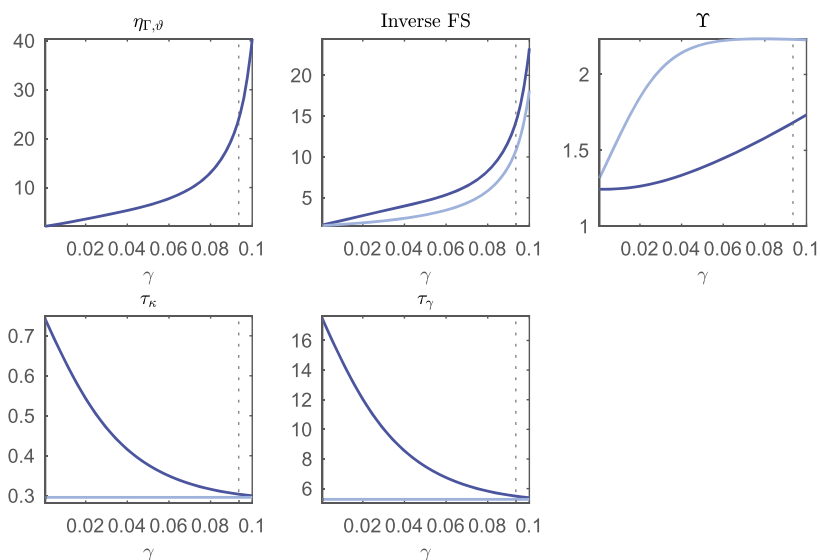
<sup>37</sup> The vertical solid line in Panels C and D is too close to the horizontal axis to be visible.

<sup>38</sup> Numerically, the statistics in the first row of the  $\kappa$  column in Table 6 is only a little smaller than the corresponding number in the last row. Presumably, this reflects a heavy penalty assigned by the principal component statistic to the plunge in  $\nu_{FS}^{NS}$  as  $\kappa$  gets small. Recall that the statistic is a function of the square of the deviation of a factor from 100. Our assessment that  $\gamma$  and  $\kappa$  are each as favorable towards the inverse FS in the non-structural decomposition reflects that we downplay somewhat the poor performance in  $\nu_{FS}^{NS}$  for small values of  $\kappa$ .



Note: the figures display the graph of  $\eta_{\Gamma, \vartheta}$  and of the elements of the two decompositions implied by Proposition 1, for the low worker share version of the AOB model (see the text for the definition of this model). The graphs show how these elements vary as the value of  $\delta$  varies over the interval,  $[0, 0.06]$ , holding the other model parameters fixed. The light curve corresponds to structural decomposition and dark curve corresponds to non-structural. The solid vertical line indicates the value  $\delta$  in the low worker surplus version of the AOB model. As the value of  $\delta$  varies over the interval,  $[0, 0.06]$ ,  $f$  varies from 0.34 to 0.78. When  $\delta = 0$  the low worker share AOB has an equilibrium, and in this case we verified that  $\tau_{\kappa}$ ,  $\tau_{\gamma}$  and  $\Upsilon$  are exactly what is predicted by equation (34) in each decomposition.

Fig. 12. Two-factor Decompositions in Low Worker Share AOB model, as a Function of  $\delta$ .

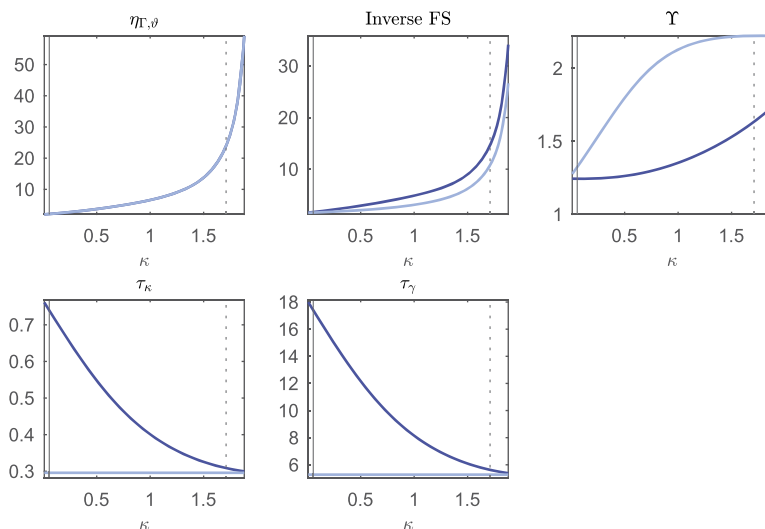


Notes: see Fig. 1. The graphs show how the two two-factor decompositions implied by Proposition 1 vary as the value of  $\gamma$  varies over the interval,  $[0, 0.1]$ , holding the other model parameters fixed. For  $\gamma$  somewhat higher than the upper bound on the grid, the elasticity rises sharply and distorts the scale in the figure. The dashed vertical line indicates the value  $\gamma$  required to obtain  $\eta_{\Gamma, \vartheta} = 24.2$  in the low worker surplus version of the AOB model. The value of  $f$  falls from 0.64 to 0.01 as  $\gamma$  rises from its lower bound to its upper bound.

Fig. 13. Two-factor decompositions in low worker share AOB model, as a function of  $\gamma$ .

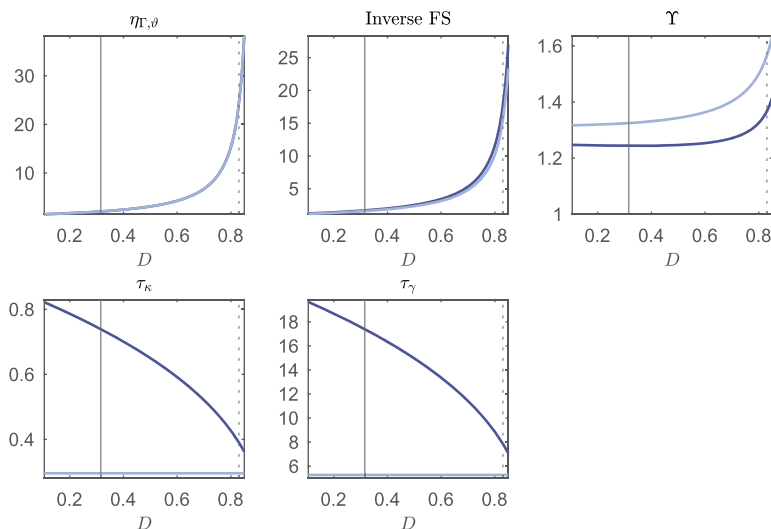
So, the results in Fig. 11 are consistent with the notion that the inverse FS in the non-structural decomposition is (weakly) best across all the factors and for the parameters that have the capacity to substantially increase the value of  $\eta_{\Gamma, \vartheta}$ .

We include Figs. 12–15 for completeness. It is interesting how similar the shape of both versions of the inverse FS is, compared to that of  $\eta_{\Gamma, \vartheta}$ . At the same time, we can see a sharp difference between these two measures of the inverse FS: in the structural case,  $\tau_{\kappa}$  and  $\tau_{\gamma}$  are constant, while these coefficients on  $\kappa$  and  $\gamma$ , respectively, are very sensitive to variations in the parameters.



Notes: see Fig. 1. The graphs show how the two two-factor decompositions implied by Proposition 1 vary as the value of  $\kappa$  varies over the interval,  $[0.01, 1.88]$ , holding the other model parameters fixed. The dashed vertical line indicates the value  $\kappa$  required to obtain  $\eta_{\Gamma, \delta} = 24.2$  in the low worker surplus version of the AOB model. The value of  $f$  falls from 0.67 to 0.01 as  $\kappa$  rises from its lower bound to its upper bound on the grid. That upper bound is selected because  $\eta_{\Gamma, \delta}$  and the inverse FS rise sharply for  $\delta$  larger than 1.88 and distorts the scale in the graphs. The solid vertical line indicates the value of  $\kappa$  in the low worker surplus version of the AOB model.

Fig. 14. Two-factor decompositions in low worker share AOB model, as a function of  $\kappa$ .



Notes: see Fig. 1. The lowest value of  $D$  corresponds to  $f = 0.94$  and the highest value of  $D$  corresponds to  $f = 0.05$ , so this is, roughly, the admissible values of  $D$  for the baseline parameterization of the AOB model in Table 1.

Fig. 15. Two-factor decompositions in low worker share AOB model, as a function of  $D$ .

**Fact 2.** Applying the principal component method to the AOB model, we obtain the following results: (1) for the estimated model the factor that best tracks the response of  $\eta_{\Gamma, \delta}$  to perturbations in the value of a parameter depends on the size of the perturbation and which parameter is considered; (2) for the estimated model we provide a scalar metric of how well factors track  $\eta_{\Gamma, \delta}$  overall, and we find that on average the inverse FS in the non-structural decomposition works best; and (3) for the low labor share version of the model, the inverse FS in the non-structural representation is more consistently the best factor, at least for the parameters that we consider and which have the capacity to substantially increase  $\eta_{\Gamma, \delta}$ .

To summarize, in an overall sense Facts 1 and 2 make a case based on the principal component method, that the inverse FS is the important channel by which a parameter operates, if it is to substantially increase  $\eta_{\Gamma, \delta}$ . But, there are two important caveats. The first one is provided by statement (2) of Fact 1. That uses the Nash model to construct an example in which the inverse FS is the factor which accounts best for the impact on  $\eta_{\Gamma, \delta}$  of parameter perturbations. But, Proposition 1

provides two measures of the FS and we show that one measure is ‘best’ in a version of the Nash model with a high value of the worker bargaining parameter,  $\eta$ , which the other measure is ‘best’ for a low value of  $\eta$ . This lack of robustness of the best measure of FS to a change in a model parameter is disconcerting, particularly because there is a substantial qualitative difference between the two measures of FS. The second caveat is conveyed by Fact 2, part (1). There we allude to the results in this section based on our estimated AOB model. These show how different factors can be ‘best’ in different regions of the parameter space and across different parameters. This also is disconcerting.

## References

- Auclert, Adrian, Rognlie, Matthew, Straub, Ludwig, 2019. Micro Jumps, Macro Humps: Monetary Policy and Business Cycles in an Estimated HANK Model. Northwestern University. Manuscript.
- Binmore, Ken, Rubenstein, Ariel, Wolinsky, Asher, 1986. The Nash bargaining solution in economic modeling. *The Rand Journal of Economics* 17 (2), Summer.
- Broer, Tobias, Hansen, Niels-Jakob H., Krusell, Per, Öberg, Erik, 2020. The new Keynesian transmission mechanism: a heterogenous-agent perspective. *The Review of Economic Studies* 87 (1), 77–101.
- Campbell, John, Cochrane, John, 1999. Force of habit: a consumption-based explanation of aggregate stock market behavior. *Journal of Political Economy* 107 (2), 205–251.
- Christiano, Lawrence J., Eichenbaum, Martin, Evans, Charles L., 2005. Nominal rigidities and the dynamic effects of a shock to monetary policy. *Journal of Political Economy* 113 (1), 1–45.
- Christiano, Lawrence J., Eichenbaum, Martin, Trabandt, Mathias, 2015. Understanding the great recession. *American Economic Journal: Macroeconomics*, *American Economic Association* 7 (1), 110–167.
- Christiano, Lawrence J., Eichenbaum, Martin, Trabandt, Mathias, 2016. Unemployment and business cycles. *Econometrica* 84, 1523–1569.
- Christiano, Lawrence J., Trabandt, Mathias, Walentin, Karl, 2011. Introducing financial frictions and unemployment into a small open economy model. *Journal of Economic Dynamics & Control* 35, 1999–2041.
- Del Negro, Marco, Eusepi, Stefano, Giannoni, Marc, Sbordone, Argia, Tambalotti, Andrea, Cocci, Matthew, Hasegawa, Raiden B., Linder, M. Henry, 2013. The FRBNY DSGE Model. No. 647, Staff reports, Federal Reserve Bank of New York.
- den Haan, Wouter, Ramey, Garey, Watson, Joel, 2000. Job destruction and propagation of shocks. *The American Economic Review* 90 (3), 482–498.
- Diamond, Peter A., 1982. Aggregate demand management in search equilibrium. *Journal of Political Economy* 90 (5), 881–894.
- Eichenbaum, Martin, Johannsen, Ben, Rebelo, Sergio, 2019. Monetary Policy and the Predictability of Nominal Exchange Rates. Unpublished manuscript.
- Fair, R., Taylor, J., 1983. Solution and maximum likelihood estimation of dynamic nonlinear rational expectations models. *Econometrica* 51 (4), 1169–1185.
- Gertler, M., Trigari, A., 2009. Unemployment fluctuations with staggered Nash wage bargaining. *Journal of Political Economy* 117 (1), 38–86.
- Hagedorn, M., Manovskii, I., 2008. The cyclical behavior of equilibrium unemployment and vacancies revisited. *The American Economic Review* 98 (4), 1692–1706.
- Hall, Robert E., 2005. Employment fluctuations with equilibrium wage stickiness. *The American Economic Review* 95 (1), 50–65.
- Hall, Robert E., Milgrom, Paul R., 2008. The limited influence of unemployment on the wage bargain. *The American Economic Review* 98 (4), 1653–1674.
- Kehoe, Patrick, Lopez, Pierlauro, Midrigan, Virgiliu, Pastorino, Elena, 2019. Asset Prices and Unemployment Fluctuations. Manuscript.
- Kollmann, Robert, 2001. The exchange rate in a dynamic-optimizing business cycle model with nominal rigidities: a quantitative investigation. *Journal of International Economics* 55 (2), 243–262.
- Ljungqvist, Lars, Sargent, Thomas J., 2017. The fundamental surplus. *The American Economic Review* 107 (9), 2630–2665.
- Ljungqvist, Lars, Sargent, Thomas J., 2021. The fundamental surplus strikes again. *Review of Economic Dynamics* 41, 38–51. This issue.
- Mortensen, Dale T., 1982. Property rights and efficiency in mating, racing, and related games. *The American Economic Review* 72 (5), 968–979.
- Mortensen, Dale T., Pissarides, Christopher A., 1994. Job creation and job destruction in the theory of unemployment. *The Review of Economic Studies* 61 (3), 397–415.
- Papetti, Andrea, 2019. Unemployment and Business Cycles in the Euro Area. European Central Bank. Manuscript.
- Pissarides, Christopher A., 1985. Short-run equilibrium dynamics of unemployment, vacancies, and real wages. *The American Economic Review* 75 (4), 676–690.
- Pissarides, Christopher A., 2009. The unemployment volatility puzzle: is wage stickiness the answer? *Econometrica* 77 (5), 1339–1369.
- Rogerson, Richard, Shimer, Robert, 2011. Search in macroeconomic models of the labor market. In: Ashenfelter, O., Card, D. (Eds.), *Handbook of Labor Economics*. Elsevier, pp. 619–700. Chapter 7.
- Schmitt-Grohé, Stephanie, Uribe, Martín, 2016. Downward nominal wage rigidity, currency pegs, and involuntary unemployment. *Journal of Political Economy* 124 (4), 1466–1514.
- Shimer, Robert, 2005. The cyclical behavior of equilibrium unemployment and vacancies. *The American Economic Review* 95 (1), 25–49.
- Smets, Frank, Wouters, Rafael, 2007. Shocks and frictions in U.S. business cycles: a Bayesian DSGE approach. *The American Economic Review* 97 (3), 586–606.